Photochemistry of iron complexes

Chen, Juan; Browne, Wesley R.

Published in:
Coordination Chemistry Reviews

DOI:
10.1016/j.ccr.2018.06.008

Publication date:
2018

Coordination Chemistry Reviews 374 (2018) 15–35

Contents lists available at ScienceDirect

Coordination Chemistry Reviews

journal homepage: www.elsevier.com/locate/ccr

Review

Photochemistry of iron complexes

Juan Chen, Wesley R. Browne *

Molecular Inorganic Chemistry, Stratingh Institute for Chemistry, University of Groningen, Nijenborgh 4, 9747AG Groningen, The Netherlands

ARTICLE INFO

Article history:
Received 10 May 2018
Accepted 12 June 2018
Available online 4 July 2018

Keywords:
Iron
Photochemistry
Photoreduction
Photooxidation
Photocatalysis

ABSTRACT

Although iron is among the most abundant of the bio-essential transition metals and its coordination chemistry is of central importance to bio-inorganic and bioinspired chemistry, its photochemistry has been overshadowed by ruthenium polypyridyl complexes since the 1970s. The photochemistry of iron complexes is nevertheless rich and presents a multitude of opportunities in a wide range of fields. Here, we review the state of the art and especially recent progress in the photochemistry of iron complexes, focusing on aspects of relevance to environmental, biological and photocatalytic chemistry.

Contents

1. Introduction

Photochemistry is a small but essential branch of chemistry, recognized for example, as the basis for the "molecular machines" honored by the 2016 Nobel prize for chemistry [1,2], and is central to most life on this planet. At its most basic level, photochemistry is the conversion of electromagnetic radiation to chemical energy [3] and enables induction of chemical transformations with spatial and temporal control [1]. The chemical transformations and changes in reactivity form the basis of "photodynamic therapy" treatments in medicine [4] and in photo(redox)catalysis [5], and

* Corresponding author.
E-mail address: w.r.browne@rug.nl (W.R. Browne).

https://doi.org/10.1016/j.ccr.2018.06.008
0010-8545/

hence exploring new photochemical processes in both organic and inorganic molecular systems opens opportunities in medicine, materials and chemical reactivity.

The range of organic and inorganic compounds of interest to photochemistry is limited due primarily to the requirement that an accessible electronically excited state is either dissociative or is sufficiently long-lived to engage in energy or electron transfer, or to react with other compounds [6]. From an inorganic perspective, this demand has mostly limited attention to transition metal complexes such as those of chromium, ruthenium, and iridium [7,8]. In the case of iron complexes, the lowest excited states are metal centered (e.g., $e_g \leftarrow t_{2g}$) and are displaced with respect to the ground state facilitating rapid radiationless deactivation, and hence quenching photochemical reactivity. Nevertheless there are iron complexes that show significant photochemistry, but the design of new photoreactive complexes presents the challenge of identifying and understanding the approaches available to achieving photoreactivity. In this review, we will discuss the known photochemistry of iron complexes and categorize the various reaction classes to build a picture of the state of the art.

The reported iron complexes are mostly coordinated with organic ligands in an octahedral or, less often, tetrahedral coordination environment and the photochemistry reported to date correlates with formal oxidation state, spin state, as well as the ligand structure. Hence, we will begin our discussion by introducing electronic structures and the electronic configurations of iron complexes in their various oxidation states.

The earliest, and perhaps the best-documented, photochemical reactions are the photo-assisted Fenton and photo-induced decarboxylation reactions, both of which are of relevance to environmental and materials science (see Section 3.1 and Section 3.2). The photochemically induced release of small molecules, a field of growing importance, is dominated by:

- The release of N_2, for example, from porphyrin-ligated Fe^{III} azide complexes used to generate high valent iron complexes.
- H_2 evolution, for example, through reductive elimination from Fe-hydride complexes, which holds potential in energy storage.
- CO-release, mainly from Fe-CO complexes, which is of importance in CO-related cytoprotection, anti-inflammation, and vasodilatory therapeutic treatments.

Iron is a bio-essential element and its complexes are well recognized as candidates in photometallodrugs in cancer treatment, specifically DNA cleavage and photocytotoxicity as shown by the series of iron complexes discussed in Section 3.4. Last but not least, photocatalytic reactions using iron complexes are seeing increasing attention, with both heme and non-heme iron complexes as photo-catalysts in the oxidation of organic substrates. This area is discussed in the final section of this review.

2. Electronic structures and photophysics in iron complexes

The known oxidation states of iron range from Fe^0 to Fe^{VI}, all of which have been observed experimentally. Its cations have dominated the field of transition metal oxidation chemistry, due to its great importance in both bioinorganic and synthetic chemistry. The chemistry of iron is enriched by the number of accessible spin states; including high-, intermediate-, and low-spin iron complexes. In bioinorganic and biomimetic chemistry, the majority of iron complexes are in an octahedral or pseudo-octahedral environment. Scheme 1 illustrates the energetic ordering of the d orbitals and the electronic configurations of the oxidation states from Fe^{II} to Fe^{IV} in octahedral environments. Fe^0, Fe^V, and Fe^{VI} are not included due to the lack of reports on photoactivity of their complexes. Low-spin Fe^{II} complexes are the only diamagnetic members of this series of possible oxidation and spin states with the rest

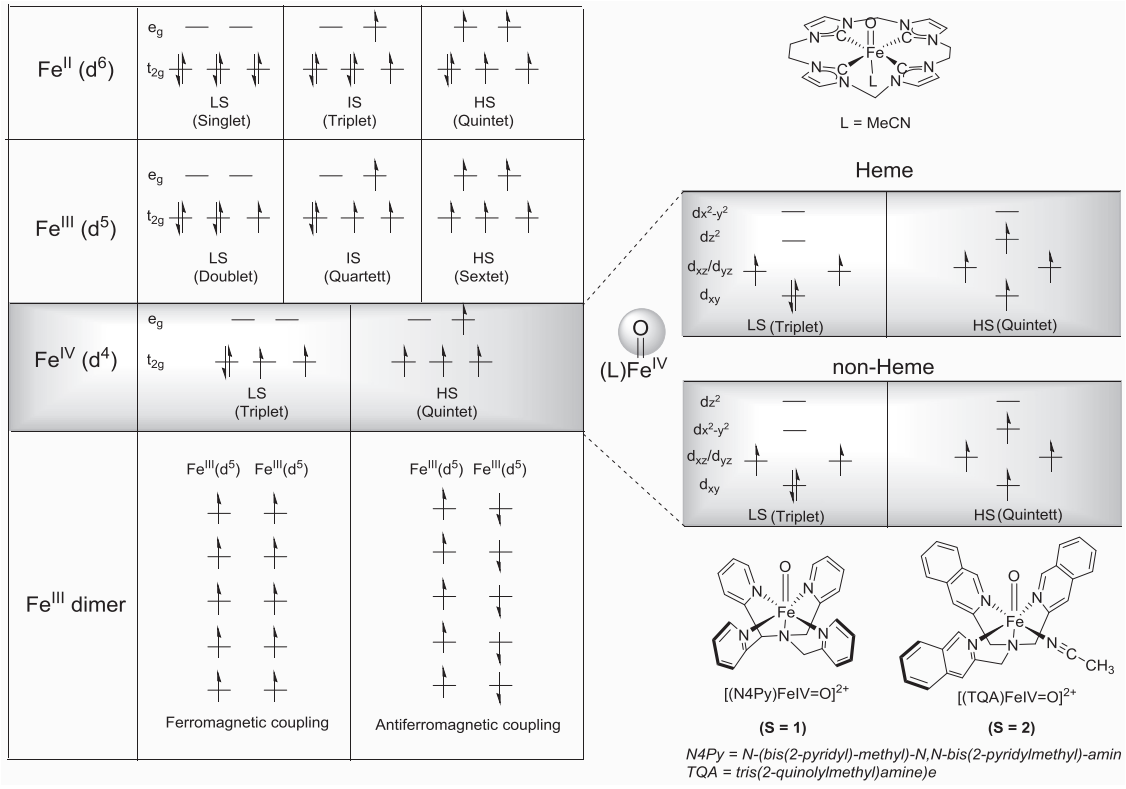

Scheme 1. (left) Oxidation and spin states of iron complexes in an octahedral geometry and (right) the ground state occupation of d-orbitals of oxo-iron(IV) complexes in pseudo-octahedral geometry for non-heme and heme complexes (structures shown are the representative for each class).

being paramagnetic. Amongst the paramagnetic states, there is a special case: the antiferromagnetic coupled arrangement of the Fe^{III} dimer, in which there are five alpha d electrons on one Fe^{III} ion and five beta d electrons on the other. In a pseudo-octahedral complex, the degeneracy of the t_{2g} and e_g orbitals (Scheme 1 left) is lifted further (Scheme 1 right). For example, in oxo-iron(IV) complexes the five d orbitals are different in energy, and the ligands can change the energy ordering of the orbitals; the $d_{x^2-y^2}$ orbitals are higher in energy than the d_{z^2} in a heme ligand environment (e.g., a tetracarbene – iron(IV)oxo complex in Scheme 1) [9] and *vice versa* in most of the non-heme ligand environments (e.g., N4Py, TQA) [10]. In non-heme oxo-iron(IV) complexes, the ligand also has dramatic influence on the electron configuration (spin sates). Although most of the reported non-heme oxo-iron(IV) complexes are in low-spin state (S = 1, e.g., $[(N4Py)Fe^{IV}=O]^{2+}$) [11], there are a few examples that are in a high-spin state (S = 2) with a trigonal-bipyramidal geometry [12,13]. $[(TQA)Fe^{IV}=O]^{2+}$ is the only reported pseudo-octahedral oxo-iron(IV) complex with high-spin (S = 2) ground state [14].

The photochemistry of iron complexes was studied extensively prior to the 1970s, but has been overshadowed by the photophysics and chemistry of ruthenium(II) polypridyl complexes for which hundreds of variants are known [15]. The long lived excited states observed in the latter provide ample opportunity to engage in photo-redox and other uni- and bi-molecular chemical reactions. Scheme 2a shows possible transitions in an octahedral ligand environment, including metal-centered (MC), ligand centered (LC), ligand to metal (LMCT), and metal to ligand charge transfer (MLCT). Compared to their ruthenium analogs, the energy gap between the t_{2g} and e_g orbitals is much less for iron complexes bringing the ^{3}MC state lower in energy than the other possible excited states. Hence, the lifetime of the charge transfer states are in the sub picosecond domain in iron complexes [16] compared to the microsecond lifetimes observed in ruthenium complexes, e.g., the ^{3}MLCT excited state lifetime of $[Ru(bpy)_3]^{2+}$ is 1 μs [17,18] and for $[Fe(bpy)_3]^{2+}$ it is <150 fs [19].

Recent efforts [20,21] to increase the lifetime of the ^{3}MLCT states of iron complexes has focused on increasing the ligand field strength (and hence raising the ^{3}MC states' energies) through the use of strong σ-donor ligands such as N-heterocyclic carbenes (NHC). This approach has lead to an increase in ^{3}MLCT lifetime to a few tens of picoseconds in several iron(II) complexes. Notably, Pavel and co-workers recently reported a low-spin Fe(III) complex with a relatively long lived (~100 ps) doublet ligand to metal charge transfer state (^{2}LMCT) at room temperature [16], achieved using a strong σ-donor and π-acceptor NHC ligand (Scheme 2). The ~100 ps lifetime, although short, is promising as it is sufficient to engage in photochemical processes together with the spin-allowed radiative decay to the ground state.

It is worth noting the earlier work of Toftlund, McGarvey and co-workers on the photochemistry of iron(II) polypyridyl complexes in which population of the ^{3}MC excited states lead to ligand dissociation with recovery on the late nanosecond timescale. The photochemistry described in the last section of this review shows that long lived excited states are not necessarily essential to achieve useful photochemical reactivity and instead photo-induced generation of reactive species is of relevance also [22].

3. Photochemistry of iron complexes

Although exciting progress is being made in controlling the photophysical properties of iron complexes, their excited state properties remain largely underexplored in comparison to their ruthenium and osmium analogs. This, however, is not to say that the photochemistry of iron complexes is limited. Indeed, iron complexes show a rich and diverse range of photochemically induced reactions, including photo-assisted Fenton Reactions, photo-induced ligand degradation-decarboxylation and release of small molecules.

3.1. Photo-assisted Fenton Reactions

The photo-assisted Fenton reaction is one of earliest examples of the photochemistry of iron complexes reported [23–25]. The Fenton (H_2O_2/Fe^{II}) [24,26] or Fenton like (H_2O_2/Fe^{III}) reaction, are well known reactions, which are used mainly to generate reactive oxygen species ($HO^{\cdot}$ and $HOO^{\cdot}$) with H_2O as by-product and are used widely in the treatment of waste water [27–30]. The production of hydroxyl radicals ($HO^{\cdot}$) is strongly accelerated under UV irradiation due to the rapid regeneration of Fe^{2+} through photo-reduction of $Fe(OH)^{2+}$. It should be noted that reactions 1-(1, 2, 3), shown below, are not the only reactions involved, and that the mechanisms by which these reactions proceed are still under

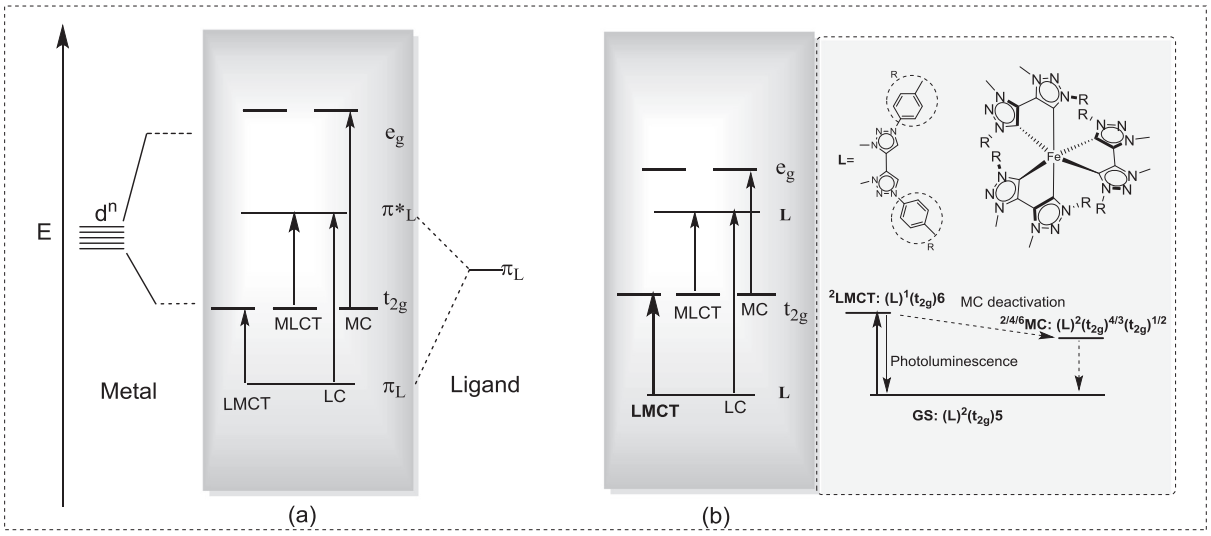

Scheme 2. (a) Jablonski diagram showing disposition of metal and ligand orbitals and possible electronic transitions for an octahedral ligand field complex, (b) Electronic transitions for low-spin d^5 iron(III) complexes [16].

debate, due in part to the possible direct photolysis of H_2O_2, as well as, the indistinguishability of Fe^{4+} and $\{Fe^{3+}(HO^{\cdot})\}$ [26].

$$Fe^{2+}H_2O_2 \rightarrow Fe^{3+}HO^{\cdot} + OH^{-} \quad (1\text{-}1)$$

$$Fe^{3+}H_2O_2 \rightarrow Fe^{2+}HOO^{\cdot} + H^{+} \quad (1\text{-}2)$$

$$Fe(OH)^{2+} \xrightarrow{h\nu} Fe^{2+}HO^{\cdot} \quad (1\text{-}3)$$

3.2. Photo-induced ligand degradation – decarboxylation

The photochemical activity of Fe^{III} carboxylato complexes, is generally more pronounced than the solvated Fe^{III} ion, due to the possibility of metal to ligand charge transfer (LMCT) excitations in the former. LMCT excitation results in the transient reduction of the iron center and can lead to oxidative degradation of the organic ligand [31–34]. Fig. 1 shows one of the most famous examples of such photochemistry, the ferrioxalato complex. The photo-induced reduction of ferrioxalate was first reported by Parker in 1953 [35], followed by a report of similar photochemical activity in iron complexes bearing a carboxylato group in their ligand structures (Fig. 2) [32,34,36]. Among the carboxylato ligands reported, the ferrioxalato complex is used widely as an actinometer in quantum yield determinations [37]. The mechanism of this photoreduction, which is accompanied by degradation of the carboxylato ligand, was studied with pump/probe transient absorption spectroscopy and quantum chemical simulations by several groups [38–42]. There are two mechanistic aspects still under discussion; especially the steps immediately following the photoexcitation. Pozdnyakov et al. proposed that intramolecular charge transfer from oxalate ligand to the Fe^{III} center results in reduction to Fe^{II}, which is in contrast to that proposed earlier by Rentzepis and co-workers in which the Fe^{III}–O bond cleaves before electron transfer. The recent advances in ultrafast high resolution transient spectroscopy have enabled reexamination of this reaction. In 2017, the Gilbert and co-workers [38] proposed a mechanism based on direct spectroscopic evidence for the first step in this photolysis reaction (Fig. 1). Electron transfer occurs within 0.1 ps of photoexcitation and results in the formation of an intermediate ferrioxalate radical anion, which then dissociates rapidly to form thermally excited CO_2 and $CO_2^{\cdot-}$. The CO_2 relaxes and then leaves the Fe^{II} center whereas the $CO_2^{\cdot-}$ radical anion remains coordinated for ~10 ns.

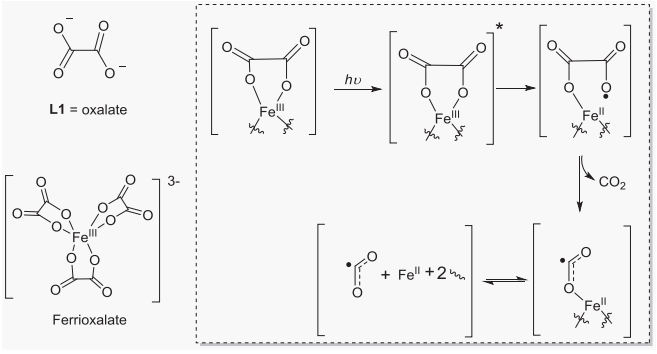

Fig. 1. Proposed pathways for photo-induced ligand degradation of ferrioxalate. For clarity, two of the oxalate ligands are omitted [36,38].

The photochemistry of Fe^{III}-carboxylato complexes in aqueous solutions is highly dependent on the ligand environment [43]. As for oxalate (L1), di-carboxylato ligands, such as succinate (L5), citrate (L8), and glutarate (L10), coordinate strongly to Fe^{III} centers, and their complexes show strong LMCT absorption bands. Photolysis mostly follows the mechanism shown in Fig. 1. In contrast, complexes of mono-carboxylate ligands, 2-propanoate (L2), 2-oxoacetate (L3), and gluconate (L9), show a dependence of the photo reaction on ligand concentration, because the carboxylato-complexed Fe^{III} complex is in equilibrium with $Fe^{III}(OH)$ species. At low ligand concentration, the photolysis of $Fe^{III}(OH)$ dominates, and produces ·OH primarily (Eq. 1-(1–3)).

The photo-induced decarboxylation of Fe^{III} complexes bearing carboxylato groups (L1-L10) is of substantial importance in the treatment of environmental pollutants. Indeed small carboxylate compounds are abundant on earth and frequently invoked in biogeochemical cycles [43–46]. Attention has been directed to ligands of the type L11 over the last decades due to their potential application in catalytic oxidations and structural variability [47]. The polypyridine amine based tripodal amine chelated Fe^{III} complex, $[(L_{11})Fe^{III}\text{-}X]$, with a carboxylato moiety undergoes ligand decarboxylation under UV irradiation concomitant with reduction of Fe^{III} ion to Fe^{II} (Fig. 3) [47].

Siderophores are a wide range of compounds produced by bacteria. They bear the α-hydroxy carboxylic acid functionality and coordinate readily to Fe^{III} ions enabling the passive uptake of iron. Recently, Butler and co-workers [48,49] showed that Fe(III)-siderophore complexes containing an α-hydroxy acid group can undergo photo-induced decarboxylation. Ligand to metal charge transfer excitation upon UV irradiation results in decarboxylation and oxidation of the petrobactin ligand to form a new ligand (loss of the central carboxylic acid group with a 3-ketoglutarate group or an enol group remaining on the original citrate backbone, Fig. 3). Indeed the photochemistry of siderophore-like Fe^{III} complexes

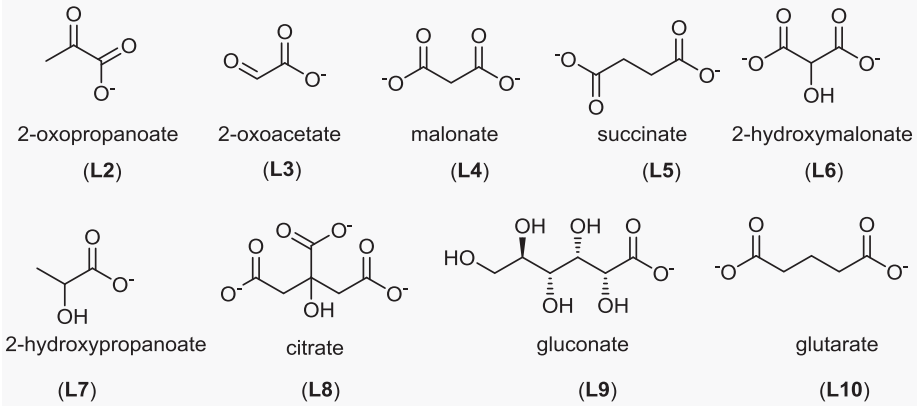

Fig. 2. Structures of carboxylate ligands mentioned in the text.

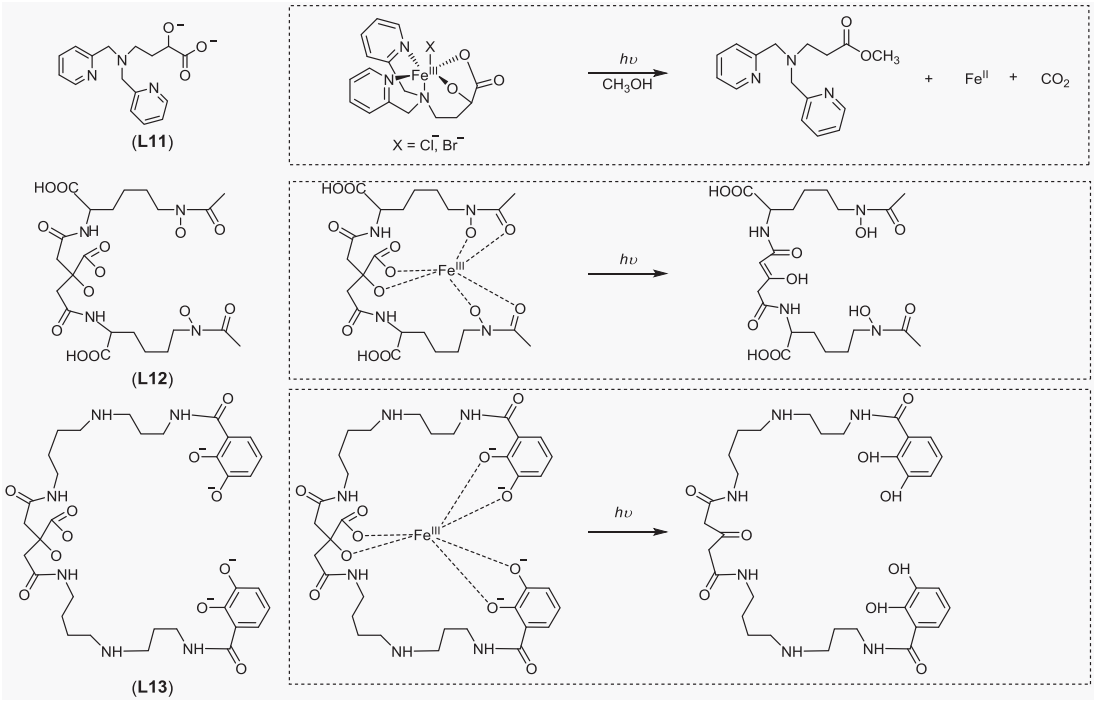

Fig. 3. Examples of ligand decarboxylation in Fe^{III} complexes under irradiation [47,48,50].

(L12, L13) is important in the transportation of iron in vivo for phytoplanktonic communities [49].

Melman and co-workers applied photo-induced decarboxylation in Fe^{III} complexes to achieve gel-sol transitions of a hydrogel with UV or visible light [51]. The hydrogels consist of alginate cross-linked with iron(III) cations. In the presence of sacrificial hydroxy carboxylates, irradiation leads to photoreduction of the Fe(III) ions to Fe(II). This change in redox state results in dissociation from the alginate, and hence a loss of crosslinking that induces a gel-sol transition of the hydrogel. Later Ostrowski and co-workers [52] developed this approach without the use of sacrificial components, using hydrogels consisting of Fe(III) ions and the polysaccharides poly[guluronan-co-mannuronan] (alginate, L14) or poly[galacturonan] (pectate, L15), (Fig. 4). Notably, they observed that the photoreactivity was dependent on the configuration of the chiral center bound to the iron ions, which provides additional control over the stability and photoresponse of metal-coordinated materials, and is of importance for broader application to biological and tissue engineering [53–55].

3.3. Photo-induced release of small molecules

The release of small molecules, especially NO and CO, are of contemporary interest due to the biological activity of such compounds and especially their role in cellular signaling. The generally low toxicity of iron complexes is attractive in the development of therapeutics in which these small molecules are released upon irradiation, and hence can be released locally.

3.3.1. Photo-induced N-N cleavage – N_2 release

Wagner and Nakamoto noted, already in 1989, the photo-induced release of N_2 from a porphyrin-ligated (L16-17) Fe^{III} azide complex (thin film) under irradiation with UV–visible (406.7–514.5 nm) light in frozen dichloromethane (30 K) [56]. Photo-induced heterolytic cleavage of the N—N bond was accompanied by oxidation of the iron center to form an iron nitrido complex $(L)Fe^{V}{\equiv}N$ with concomitant release of N_2 (Fig. 5). The formation of the $(L)Fe^{V}{\equiv}N$ complex was confirmed by resonance Raman spectroscopy with the ν(Fe—N) band at 876 cm^{-1} and 873 cm^{-1} for (L16, L18)$Fe^{V}{\equiv}N$ and (L17)$Fe^{V}{\equiv}N$, respectively [56]. Due to the substantial electron deficiency of $(L)Fe^{V}{\equiv}N$, the photochemistry could only be studied in a cryogenic inert matrix or thin film. As with the non-innocence of the porphyrin ligand in oxo-iron(IV) enzymes (P450 compound I) [57], the d^3-iron(V) center with a closed shell dianionic ligand is a resonance structure of a d^4-configured iron(IV) center with the ligand radical monoanion by virtue of magnetic coupling. Hence, the possibility of similar photolysis in redox-innocent non-heme ligand environment is challenging.

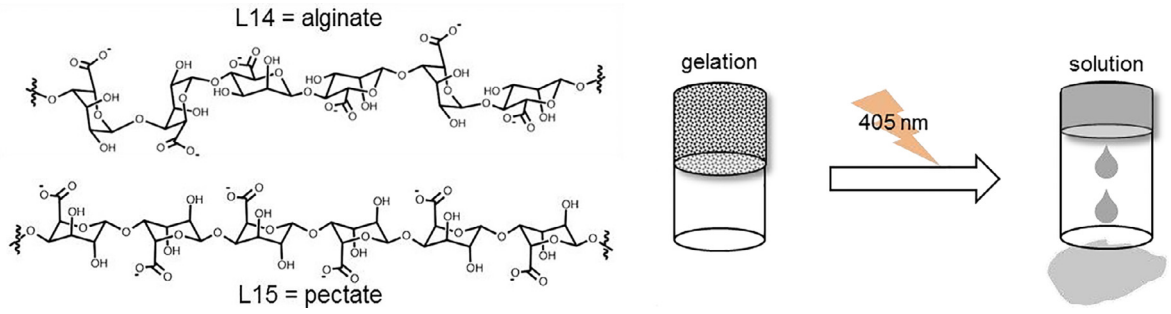

Fig. 4. Examples of gel-solution transition utilizing a photo-induced Fe^{III}-decarboxylation (adapted from [52]. Copyright ACS).

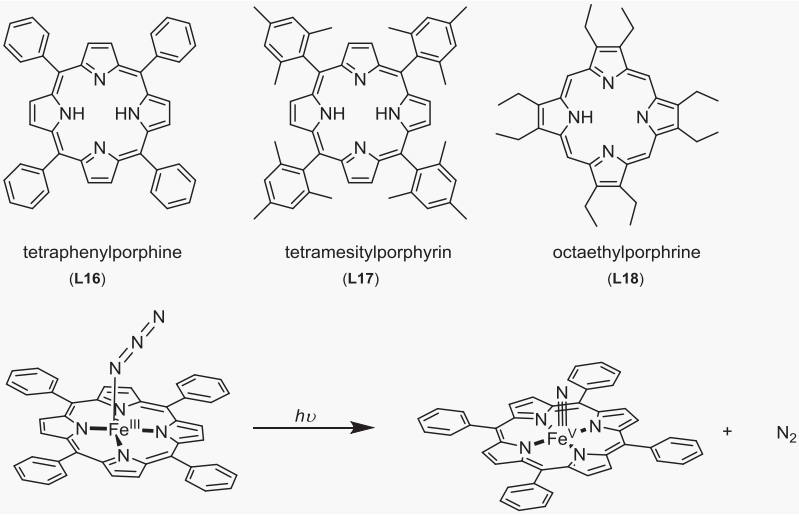

Fig. 5. Examples of photo-induced oxidation of porphyrin-ligated Fe^{III} azide complex induced by the release of N_2.

The photo-induced cleavage of a N—N bond in a non-heme iron complex was first reported by Wieghardt and co-workers (L19, Fig. 6) [58], in which the Fe^{III} center was located in a pseudo-octahedral coordination environment with azide ligands at its axial positions and four equatorial sites occupied by a redox-innocent macrocyclic ligand. High valent Fe^{V} intermediates were observed at 4 and 77 K by EPR and Mössbauer spectroscopy. In contrast to heme systems, a five-coordinate ferrous species has also been observed in the same reaction, which originates from homolytic cleavage of the Fe—N bond. Although the details of the photochemical mechanism are not established, femtosecond mid-infrared spectroscopy provides insight into the overall dynamics of the photo-induced release of N_2 and formation of Fe^{V} [59–62]. Excitation of the Fe^{III} azide precursor at 266 nm results in mainly non-adiabatic cooling (internal conversion, vibrational relaxation), resulting in full conversion of electronic energy to thermal energy. The "productive" channel of N-N cleavage and buildup of the iron (V) product are due to intramolecular vibrational energy redistribution which corresponds to the azide-associated low frequency modes, leading to N-N cleavage. Furthermore, due to the relatively high barrier for rebound between Fe^{V}/N_2 to Fe^{III}/N_3, the formed dinitrogen escapes the reaction cage readily [59].

The photolysis pathways are highly dependent on reaction conditions and ligand environment. Vöhringer and co-workers [60] found, in contrast to the studies in cryogenic inert matrices [64], that irradiation of an Fe^{III} azide precursor (L20), with one nitrogen atom replaced by an acetate group in an axial position trans to the N_3 group, almost exclusively forms the solvent-stabilized ferrous

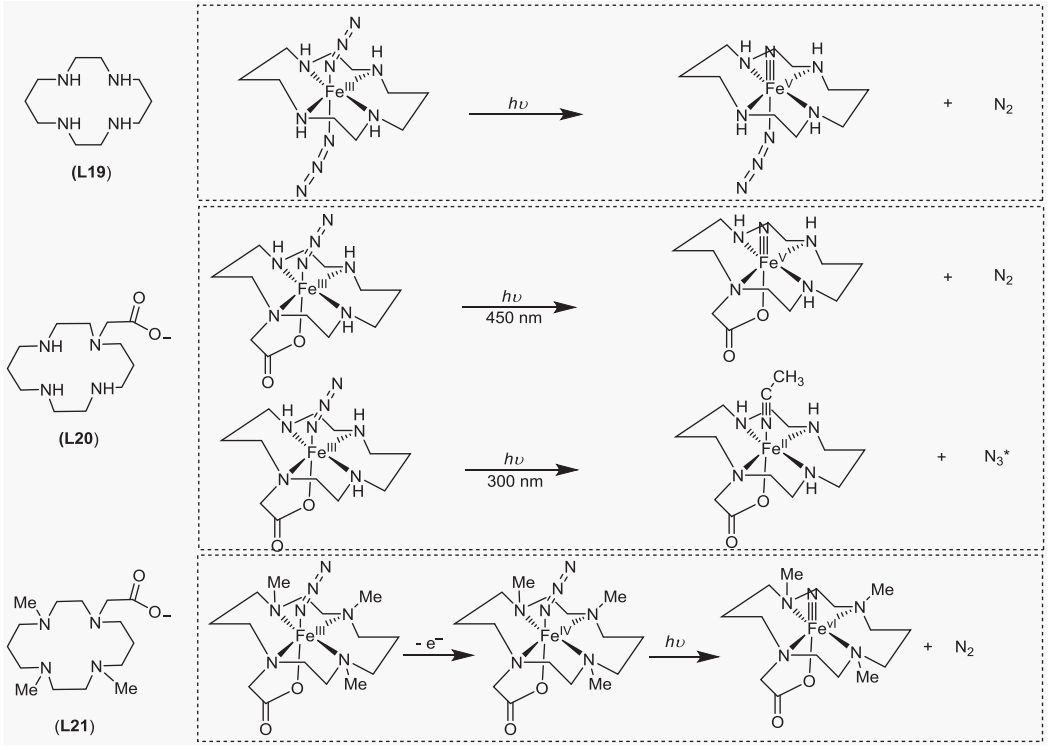

Fig. 6. Examples of photo-induced oxidation (or reduction) of non-heme Fe^{III} azide complexes with a release of N_2 [58–60,63].

complex by Fe-N cleavage at 266 nm in acetonitrile at room temperature [60]. Ferryl complex L21, generated electrochemically from ferric states, undergoes similar N-N cleavage with evolution of N_2 under irradiation at 650 nm at 77 K with formation of (L21) $Fe^{VI}\equiv N$, which is the only identified Fe^{VI} complex to date [63].

Only a few illustrative examples of the photolysis of Fe-N_3 complexes were discussed in this section but there are an increasing number of ligands developed, incorporating, for example, pyridine moieties into the amine-based ligand backbone by Costas and co-workers [65,66], which show similar photoreactivity to the complexes discussed above. It should be noted that, to date, photo-induced N-N cleavage is still the most common route to convert Fe^{III}-azido precursors to high-valent Fe^{V} or Fe^{VI} complexes, with only a few reports of thermal reactions yielding these species [61].

3.3.2. Photo-induced displacement of labile ligands – CO release

Carbon monoxide (CO) is a key molecule in biochemistry; in vivo, it is a natural metabolite and produced mainly by heme oxygenase-1 [67,68]. Certain levels of CO have a positive biochemical effect; including cytoprotection, anti-inflammation, and vasodilation, and it is often used in therapeutic treatments [69]. However, due to the high affinity for the iron center of hemoglobin, excess CO can shut down oxygen transportation [70]. Hence, the controlled release of CO from carbon monoxide releasing molecules (CORMS) is a promising strategy in the targeted delivery of CO to tissues.

Metal-CO complexes have seen the most attention due to propensity for cleavage of the M–CO bond with release of CO under irradiation. There are several recent reviews published on this topic [71–76] and here the field will be mentioned only briefly. Iron complexes are particularly attractive in CORM studies due to the low toxicity of iron, and in this section we focus on the reported Fe-CO photoCORMs.

The first Fe-CO photoCORMs for biological applications was reported by Motterlini and co-workers in 2002 [75]. However, iron pentacarbonyl, $[Fe^0(CO)_5]$, which also shows photo-induced release of CO, and its related complexes were reported prior to the 1970s [77,78]. Exposure of $[Fe^0(CO)_5]$ to a cold light source results in the release of CO, quantified using the conversion of deoxymyoglobin to carbonmonoxymyoglobin. The mechanism of photolysis was studied using picosecond and nanosecond time-resolved infrared spectroscopy by George and co-workers [79]. CO release proceeds in a step-wise manner, accompanied by a change in the symmetry of the complex. For example, at low temperature (<20 K), one CO is released to form a C_{2v} symmetric Fe $(CO)_4$, with prolonged irradiation resulting in the release of second CO to form $Fe(CO)_3$. The formed $Fe(CO)_3$ and $Fe(CO)_4$ can recombine with CO or the matrix molecules, (e.g., CH_4, Xe) depending on the irradiation conditions [79–83]. Other ligands have been incorporated into Fe-CO complexes to control the steric and electronic properties at the iron centre. Lynam and co-workers [84] developed a series of tricarbonyl complexes containing 2-pyrone ligands ($L22_{CO}$-2). Tuning the substitution on the backbone significantly affects CO release [84]. In 2010, Westerhausen and co-workers reported a biogenic dicarbonyl bis(aminoethylthiolato) iron(II) complex($L22_{CO}$-3) (Fig. 7a), which shows advantages in regard to therapeutic applications. It is soluble in water, and the CO release is triggered by irradiation with visible light ($\lambda > 400$ nm). The complex shows minor adverse effects in physiological tests [85]. Later, inspired by hydrogenases [86], which release H_2, complexes $L22_{CO}$-4 and $L22_{CO}$-5 [87–91] containing diiron centres bearing thiolate ligands were prepared. These complexes release CO under irradiation and generate a solvent coordinated complex (Fig. 7b). The CO-release rate is sensitive to the thiolates' structures. Complexes with two monothiolates ("open" form) show greater photoreactivity than a dithiolate coordinated complex ("closed" form) [92]. The dimercaptopropanoate-bridged diiron hexacarbonyl complex, reported by Fan and co-workers [90] shows rapid CO-release with six CO ligands disassociating within 30 min to 1 h, and forms a water soluble iron thiolate salt eventually [90]. Epithelial cell tests did not show obvious cytotoxicity. A common feature of these Fe^0 and Fe^1 complexes is that they tend to undergo full decomposition under irradiation, i.e. release all bound CO ligands. The non-heme $[(N4Py)Fe^{II}(CO)]$ complex ($L22_{CO}$-6, Fig. 7c), reported by Kodanko and co-workers [93], shows similar photo-induced CO release but with extraordinary thermal stability in aqueous solution. The polypyridyl ligand environment opens possibilities for ligand modification, taking advantage of the range of such ligands developed for oxidation catalysis over the last decades. Modification of the ligand with a peptide provides a handle by which photoCORM transportation to a target tissue can be envisaged in therapeutic applications [93].

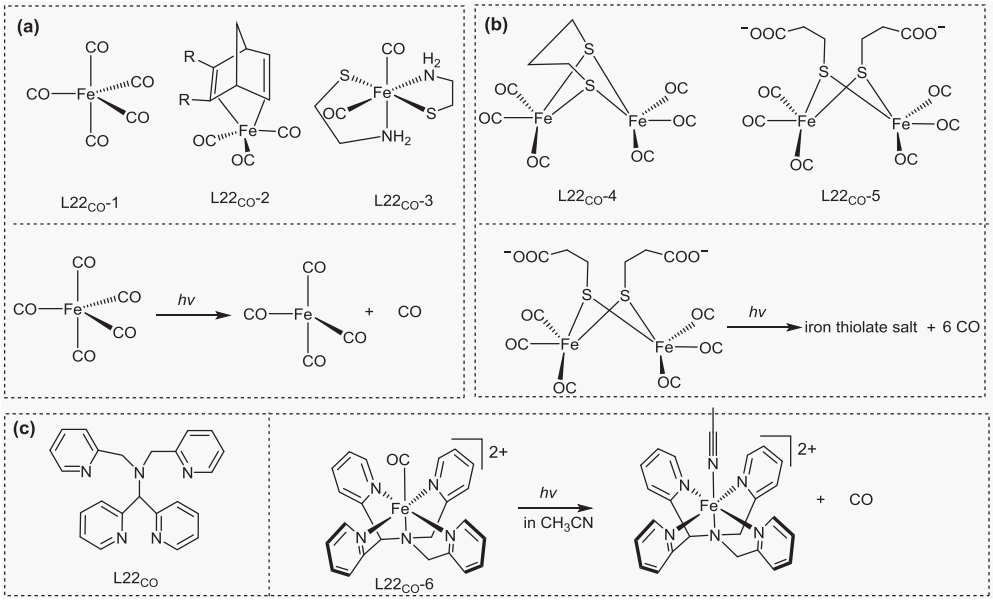

Fig. 7. Examples of photo-induced carbon monoxide releasing molecules (photoCORMs).

3.3.3. Photo-induced reductive elimination Fe-hydride – H_2 evolution

In contrast to CO-release, in which a ligand is dissociated fully, the release of H_2 is generally achieved by photo-induced reductive elimination from an Fe-hydride complex; an approach reviewed by Perutz and Procacci recently [94]. The two main classes of complexes, for which photo-induced H_2 release are observed, are monohydride and dihydride. The biomimetic hydrogenase complex ($L23_{H2}$-1), a representative example for Fe-monohydrides, was reported by Rauchfuss and co-workers [95], showed four turnovers for H_2 evolution under irradiation in the presence of triflic acid (Fig. 8a) [95].

Fe-dihydride complexes are mainly based on Fe-carbonyl (Fig. 8b) and Fe-phosphine structures (Fig. 8c). Sweany [96] noted that irradiation of $H_2Fe(CO)_4$ with a Hg lamp resulted in the appearance of a characteristic C—O stretching band (the totally symmetric mode of $Fe(CO)_4$) in matrix-isolation studies with FTIR spectroscopy. This reaction is reversed upon visible radiation (using a Nernst glower). The recombination of $Fe(CO)_4$ with the released H_2 was inferred from the reappearance of IR bands for $H_2Fe(CO)_4$. In contrast to Fe-carbonyl complexes, Fe-phosphine dihydrides show greater photo-reactivity and have been studied extensively towards the activation of strong C—H bonds under irradiation. The first step under irradiation is still the photo-reductive elimination of molecular H_2 (Fig. 8c), which leaves a vacant site on the iron centre for small molecule oxidative addition and hence C—H or C—S activation of substrates [97–99].

In addition to the above mentioned complexes, the so called "Janus intermediate", which has a redox active 4[Fe—S] core with two bridging Fe hydrides ($E_4(4H)$), was studied by Hoffman and co-workers by *in situ* EPR and ENDOR spectroscopy. This complex shows photo-induced reductive elimination of H_2 at 20 K, and reverts to ($E_4(4H)$) by oxidation of H_2 at 175 K.

3.4. Potential anticancer metallodrugs – photocytotoxicity of iron complexes

The report of cisplatin as an anticancer chemotherapeutic by Rosenberg [100] stimulated the development of several platinum-based metal complexes as metallodrugs. However, drug resistance and severe side effects stimulate the search for new non-platinum alternatives [101]. The successful application of Bleomycin [102], an iron-chelating antibiotic for cancer treatment drew attention to iron complexes and a series of biomimetic complexes with a variety of ligand environments have been reported with pre-clinical testing towards cytotoxicity in many cases [103]. Photo-activated or photodynamic treatment (PDT), in which the drug is only active under irradiation and not cytotoxic in the dark, appears to be a promising approach due to the high spatial selectivity for targeting tumors [104,105].

Achieving photo-induced DNA cleaving activity and hence photocytotoxicity with iron complexes necessitates consideration of several aspects: (a) binding of the complex to DNA, interaction with targets or related proteins for transportation, (b) transport into cells, which is closely related to the lipophilicity of the complexes, (c) high molar absorptivity in the PDT window, (d) oxidation states of the metal center that are capable of generating reactive oxygen species under irradiation. The first three properties can be addressed by ligand modification, while the last is key to the generation of reactive oxygen species and must consider the conditions encountered in vivo. As there are a number of reviews covering the cytotoxicity of iron complexes and their application in cancer treatment [103,106–108], here we focus only on recent reports of the photocytotoxicity of reported iron complexes giving

Table 1
Abbreviations of cell types mentioned in this section.

Abbreviation	Cell type	Abbreviation	Cell type
HeLa	Human cervical carcinoma,		
HaCaT	Human keratinocytes,	MCF-7	Human breast cancer
Hep G2	Human hepatocellular carcinoma	MRC-5	Human fibroblast
HPL1D	Nontransformed human epithelial lung cells	A549	Human non-small cell lung carcinoma

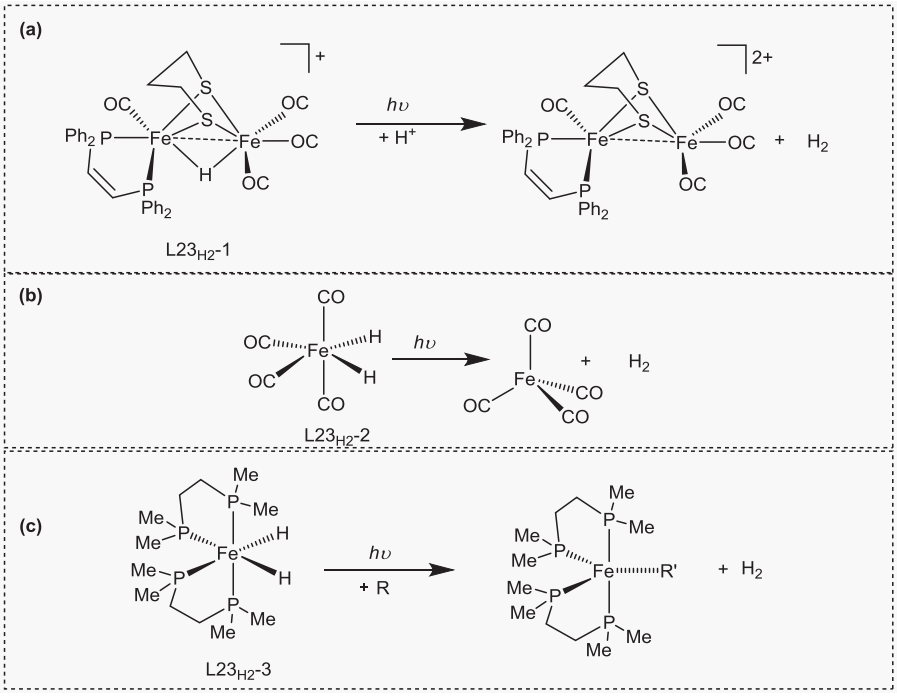

Fig. 8. Examples of photo-induced H_2 evolution by Fe-containing complexes.

representative examples rather than a comprehensive discussion of each system. Furthermore, we categorized reported iron complexes by oxidation state of the iron center here and for clarity Table 1 lists the cell lines examined in photocytotoxicity studies which are mentioned in this review.

3.4.1. Photocytotoxicity of Fe^{II} complexes

The earliest reports of photocytoxic properties of iron complexes were predominantly focused on Fe^{II} complexes (Fig. 9). Roelfes and co-workers [109] reported that the DNA cleavage activity of a polypyridyl amine-based pentadentate Fe^{II} complex (L24), which is a biomimetic model of the widely used anticancer drug Fe-Bleomycin. The DNA cleavage activity in vitro was later shown to be enhanced by irradiation with visible light. Modification of the ligand with covalently attached chromophores (L25-L28) resulted a 56-fold enhancement of the photoactivity for single-stand DNA cleavage (L25). The mechanism of DNA cleavage was originally attributed to the generation of reactive oxygen species (ROS), $HO^{\cdot}$, $O_2^{\cdot-}$, $^1O_2$, under irradiation (355, 400.8, 473 nm) [109]. In contrast to covalent attachment, the presence of chromophores (9-aminoacridine, and of 1,8-naphthalimide) did not show a synergistic effect in the photo-enhancement of the DNA cleavage activity of L24. ROS are generally accepted as the responsible agents in DNA cleavage. However, surprisingly, addition of ROS scavengers (Na_3N, DMSO and superoxide dismutase), significantly increased DNA cleavage activity under irradiation. This unexpected result revealed the complexity of the ROS mechanisms and the importance of maintaining steady-state concentrations of ROS in DNA cleavage [110]. Beyond the DNA cleavage, the photocytotoxcity of these complexes towards living cells was also studied and compared with the natural antibiotic Bleomycin; complexes L24 and L25 both show comparable efficiency in nuclear DNA cleavage with that of Bleomycin. However, the mechanisms are different. Both iron complexes induced apoptosis and not cell cycle arrest induced by mitotic catastrophe as observed with Bleomycin [111]. Apart from the pentadentate ligand bound complexes, two complexes reported recently, one bearing two planar DNA binding phenanthroline groups(L29) [112], and the other a boron dipyrromethene group attached to a NCN pincer (L30) [113], both show significant photocytotoxcity to living cells (HaCaT and MCF-7 for L29, and HeLa and MCR-5 for L30) under visible irradiation with minor dark toxicity.

3.4.2. Photocytotoxicity of Fe^{III} complexes

Several examples in which the iron(III) complexes of particular ligands show greater photo-reactivity than their corresponding iron(II) complexes have been reported. For example, the dipyridoquinoxaline (dpq) Fe^{II} complex reported by Chakravarty and coworkers is photo-inactive but its Fe^{III} complex shows significant DNA cleavage activity under visible light irradiation [114,115]. Fig. 10 shows several recently reported iron(III) complexes (Fig. 10) that engage in photo-induced DNA cleavage in different cell lines under irradiation with visible light [116–118]. The considerable number of complexes reported present certain 'design rules'. In these complexes (L31-L51), the phenolato moieties induce intense LMCT bands, which facilitates photo-irradiation and broadens the PDT window to the 620–850 nm region (L46 – L49); the bulky *tert-butyl* (in L31-L36) and hydrophilic group (-SO_3H, in L35) increase and decrease lipophilicity, respectively; planar aromatic groups increase their DNA binding affinity and act as additional photosensitizers (in L31-L36, L38, L41-L51); [119] biomarkers, e.g., biotin (vitamin H or vitamin B7, in L33 and L34) and sugars (in L37-L39) increase cytotoxic selectivity for certain cancer cell lines; [120] Schiff base pyridoxal ligands, instead of tetradentate phenolate-based ligands allow other cellular components to be targeted (e.g., the endoplasmic reticulum) (L40-L44); [121,122] As in previous studies, the cytotoxicity discussed above is due to apoptosis induced by production of reactive oxygen species upon irradiation of DNA bound complexes [123,119].

3.4.3. Photocytotoxicity of Fe^{III}-oxo bridged complexes

As a photo-metallodrug, an iron complex should have as low as possible dark toxicity to healthy cells. In contrast to the Fe^{II} and Fe^{III} oxidation states, complexes in the oxidation states Fe^0 and Fe^1 are generally unstable at ambient or physiological conditions. Complexes in the oxidation states Fe^{IV} or higher although also invoked as reactive intermediates in oxidation reactions, are not considered for PDT treatments. Diiron(III) complexes, however, are possible candidates. Fig. 11 lists a collection of diiron complexes showing photocytotoxcity.

The first report of photo-induced DNA cleavage by oxo-bridged diiron(III) complexes was by Chakravarty in 2008 [124,125], in which the almost linear Fe-O-Fe centers were coordinated by L-histidine and phenanthroline based ligands (L53-L54) (Fig. 11). These complexes display double-strand DNA cleavage under visible light irradiation. The dipyrido quinoxaline (dpq) group (L54) was proposed to bind the DNA through groove binding. Notably, the complexes were flipped when binding with DNA; the two dpq planar groups rotate via the Fe-O-Fe center to a *trans* configuration in order to reduce the steric effect of binding. In addition, in contrast to the dpq group, the phenanthroline (L53) diiron complex showed only single-strand DNA cleavage activity under visible light irradiation. Phenanthroline ligands in complexes L53 and L54 are not only the DNA binder but also the photosensitizer.

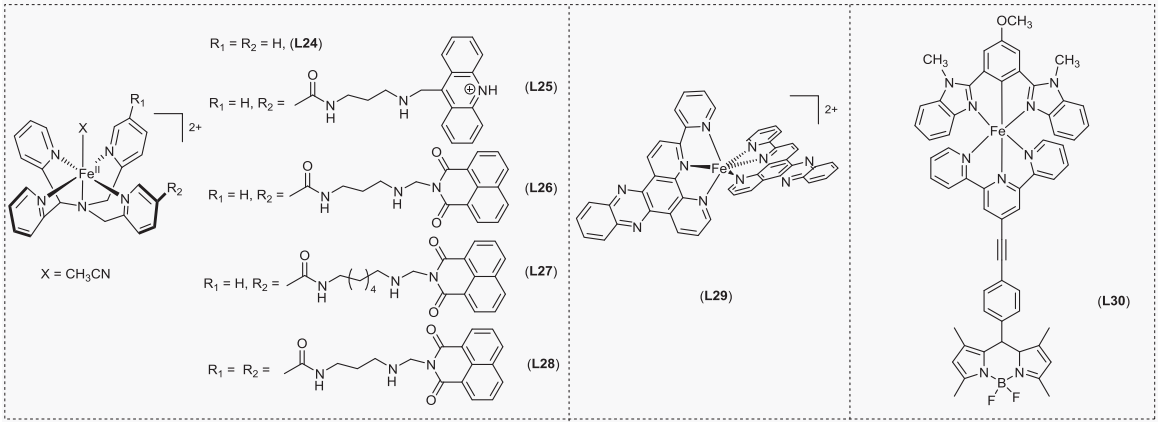

Fig. 9. Examples of Fe^{II} complexes showing photocytotoxicity.

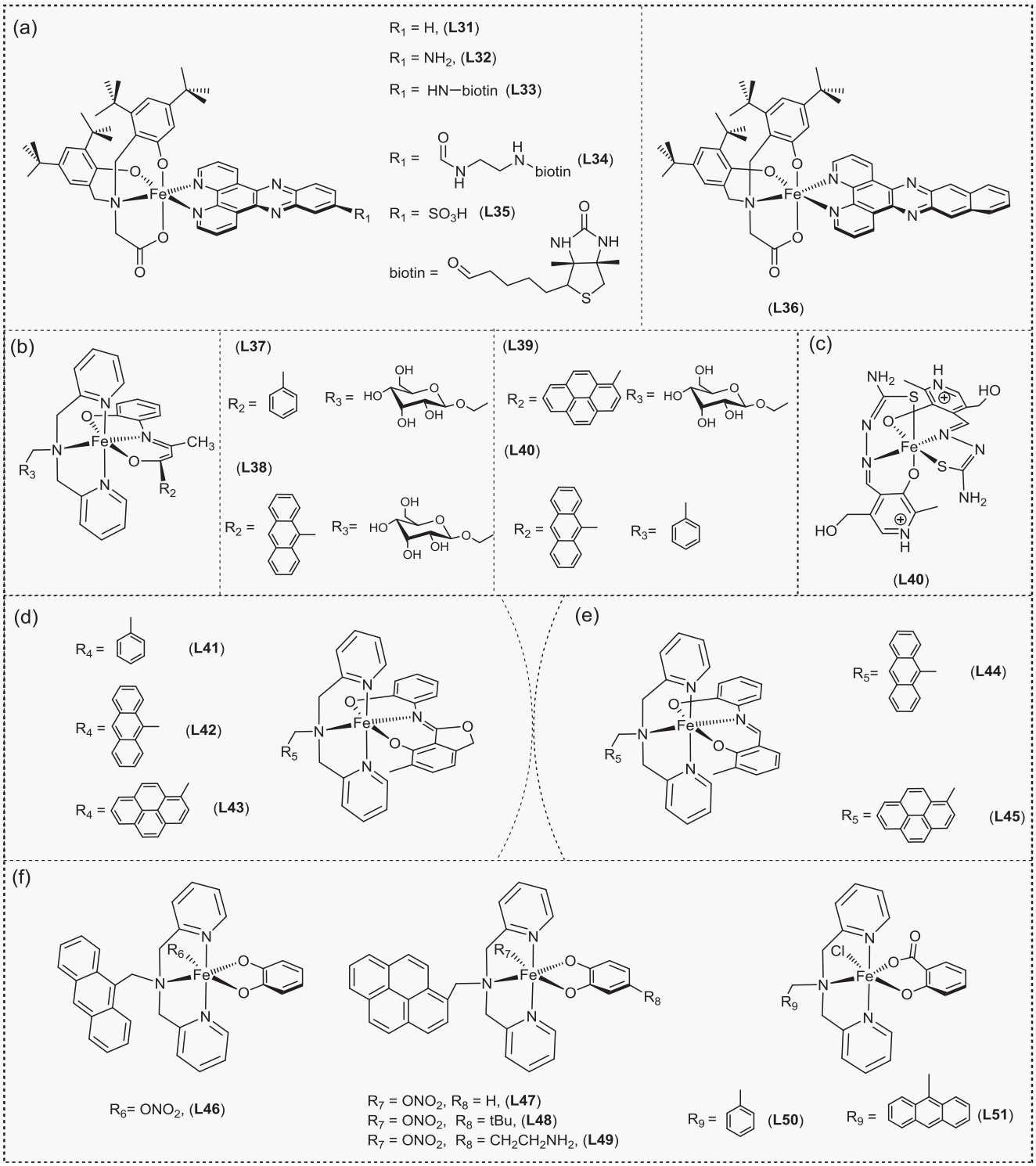

Fig. 10. Examples of Fe^{III} complexes showing photocytotoxicity.

In contrast, the complex L52, which lacks the photosensitizer, is photo-inactive towards the DNA cleavage [124]. Diiron complexes that do not have the L-histidine group but instead another dpq (L56 and L58) or phenanthroline (L55 and L57) ligand [126], bind DNA more strongly [124] than complexes L52-L54. The near linearly oxo-bridged diiron complexes, L55 and L56 are more active than the acetate bridged complexes L57 and L58. Photo-induced DNA cleavage activity is wavelength dependent for these complexes: complex L58 shows activity under red light while the other two complexes are active only at shorter wavelengths, and complex L55 is photo-inactive. The mechanism of DNA cleavage in all cases (L53, L54, L57, L58) is attributed partially to the Fe-carboxylato group present, which, see Section 3.2, under irradiation undergoes decarboxylation to produce reactive radical species that cleave DNA.

The cytotoxicity of these complexes, under specific conditions (excess H_2O_2), has been established to be greater in the case of cancer cells than in healthy cells. This difference is amplified by

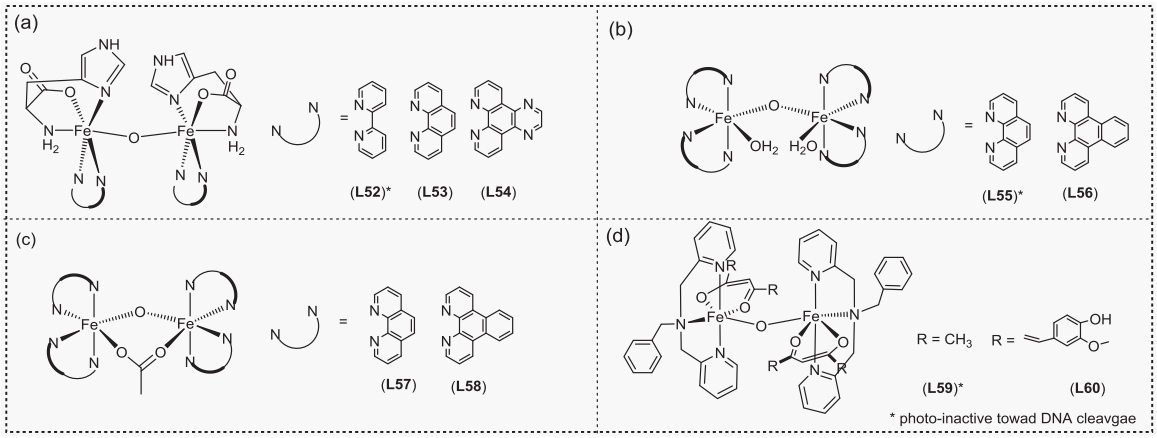

Fig. 11. Examples of diiron(III) complex showing photocytotoxicity.

irradiation with visible light [127]. The photocytotoxic diiron(III) complex (L60), which bears a curcumin unit and not a Fe^{III}-carboxylato group, shows enhanced stability and photocytotoxicity towards HeLa and MCF-7 cells under irradiation. Curcumin is proposed to be the photo-active group since the analogous complex L59 is photo-inactive [128].

As discussed above, iron is a bio-essential metal and its complexes generally show low toxicity in vivo, but can be activated to induce a variety of cellular processes leading to cell death and thereby hold potential as photo-metallodrugs, not least in the treatment of cancer. Ligand structure plays a key role in determining photocytotoxicity, and the abundance of small molecules, which are already well-documented in clinic studies for anticancer treatment or reagent transportation, could be readily incorporated into ligand structures. This increases the possibilities for the use of iron complexes as photometallodrugs in PDT. However, the mechanisms are still unclear with the lack of the information on the photo-activity of the iron complexes themselves limiting understanding of the cytotoxic mechanisms. Hence, close examination of the photoreactivity of iron complexes is essential in order to advance this field further.

3.5. Photochemistry of iron complexes in catalytic oxidations

The increase in the number and variety of organic ligands has opened many opportunities in controlling the reactivity of iron-based homogenous catalysts [129], and especially redox cooperativity between metal and ligand promises replacement of noble metals by iron. Furthermore, modern spectroscopy provides extensive information about catalyst structure and mechanism, which has enabled biomimetic approaches to ligand design. High-valent iron-oxo species are invoked as the reactive species in the oxidation of organic substrates in both enzyme and synthetic catalytic reactions frequently. There are several approaches to accessing high oxidation states, such as: sacrificial oxidants (e.g., H_2O_2, PhIO, m-CPBA etc.) [130], electrochemical oxidation [131], and photo excitation [132]. Photochemistry is advantageous due to its non-invasive and atom economic nature and is drawing more attention in recent years. In this section, we focus on the application of photochemistry in catalytic oxidations by iron complexes. The photo-induced generation of higher oxidation states or reactive oxygen species can be achieved by either of two ways: the direct excitation and the indirect excitation with the use of a photosensitizer. We will discuss briefly the second approach, despite that on first glance it appears as a trivial example of photochemistry with iron complexes since the actual photochemistry is carried out by a separate species (e.g., a ruthenium(II) complex). As will become apparent in the subsequent sections, it is likely that the sensitized systems need to be reevaluated given the intrinsic photoreactivity of the iron complexes used that was not considered in the original studies.

3.5.1. Photo-induced catalytic reaction—the use of a photosensitizer

The use of a photosensitizer to introduce extra energy to a reaction is well established, not least in the field of photoredox catalysis. In regard to iron catalysis, the most widely used photosensitizers are Ru^{II} complexes (e.g., $[Ru(bpy)_3]^{2+}$) due to their outstanding photophysical and photochemical properties. The excited state of $[Ru(bpy)_3]^{2+*}$ generated under visible light irradiation can engage in electron transfer to form $[Ru(bpy)_3]^{3+}$, which is a strong oxidant (1.26 V vs SCE, Fig. 12) and can oxidize most iron complexes to their higher oxidation states. This approach is a so-called "multi-catalyst strategy" (Fig. 12).

3.5.1.1. The application of photosensitized heme-based catalytic systems. Gray and co-workers [133] reported the photo-induced generation of high-valent metalloenzyme intermediates in a heme complex using the photosensitizer $[Ru(bpy)_3]^{2+}$ as electron donor (Fig. 13). Nanosecond transient absorption showed that excitation of $[Ru(bpy)_3]^{2+}$ to its excited state $[Ru(bpy)_3]^{2+*}$ is followed by electron transfer to $[Ru(NH_3)_6]^{3+}$ (electron acceptor, EA) to form the strong oxidant $[Ru(bpy)_3]^{3+}$. It can directly oxidize ferric microperoxidase-8 (MP8) $[(P)Fe^{III}\text{-}OH_2]$ (L59) to its cation radical ferric form $[(P^{\cdot+})Fe^{III}\text{-}OH_2]$, which is in equilibrium with the ferryl MP8 $[(P)Fe^{IV}{=}O]$ (Compound **II**). Lowering pH (pH <6) shifts the equilibrium away from the ferryl MP8 and *vice versa* [133]. Later, the same concept was applied to the heme Horseradish Peroxidase (HRP) [134], with $[Co(NH_3)_5Cl]^{2+}$ as the electron acceptor. The HRP ferryl species (Compound **II**) is formed via a ferric π-cation porphyrin radical species $[(P^{\cdot+})Fe^{III}\text{-}OH_2]$ intermediate at alkaline pH. Notably, the ferryl porphyrin radical species $[(P^{\bullet+}))Fe^{IV}{=}O]$ (Compound **I**) formed by oxidation of Compound **II** was also observed [134].

As discussed above, the rate determining step is the porphyrin-based ligand oxidation and hence this approach is unsuitable for the thiolate-ligated heme cytochromes P450 since the heme is buried deep inside the enzyme. Cheruzel and co-workers [135] reported a new strategy, in which the photosensitizer [(IA-phen) $Ru(bpy)_2]^{2+}$ (IA-phen = 5-iodoacetamino-1,10-phenanthroline) was covalently bound to cytochrome P450 BM3 (Ru^{II}_{K97C}–Fe^{III}_{P450}) (Fig. 14). Under irradiation three species with well-defined transient absorption spectra were observed, first $*Ru^{II}_{K97C}$–Fe^{III}_{P450}, second Ru^{III}_{K97C}–Fe^{III}_{P450} and returning back to the initial Ru^{II}_{K97C}–Fe^{III}_{P450}. Kinetic studies reveal three transient species assigned as Ru^{II}_{K97C}–$(P^{\cdot+})$

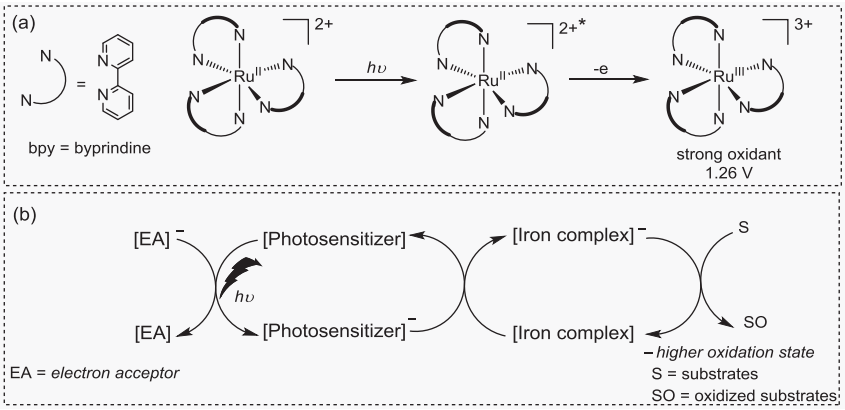

Fig. 12. Photochemistry of $[Ru(bpy)]^{2+}$ (a) and a multi-catalyst strategy in catalytic oxidation with iron complexes (b).

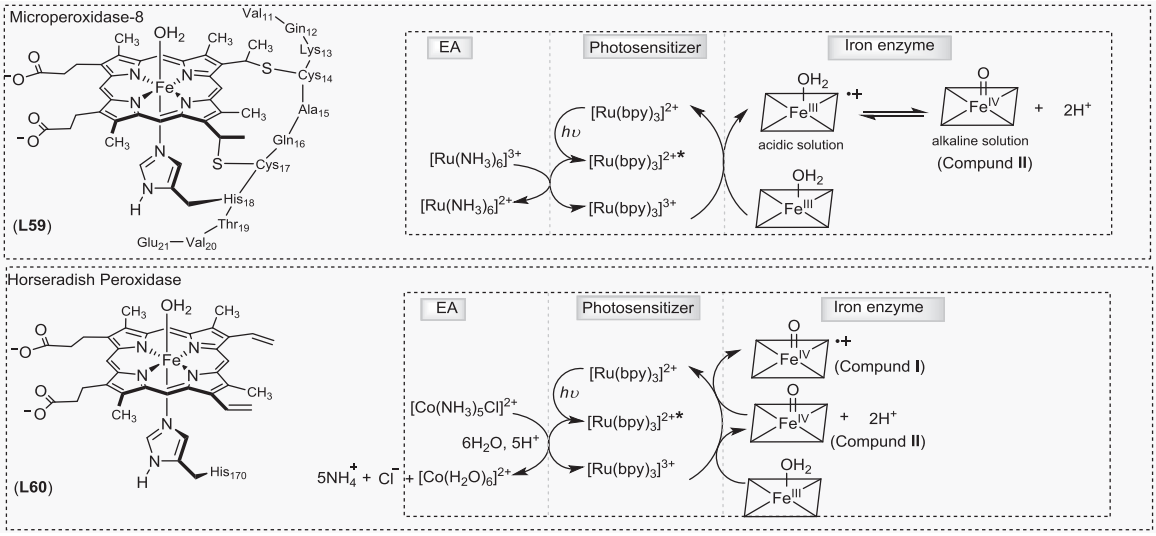

Fig. 13. Examples of generation of high-valent metalloenzymes by a multi catalyst strategy.

$Fe^{III}_{P450(A)}(OH_2)$, Ru^{II}_{K97C}–$[(P^{\cdot+})Fe^{III}_{P450(B)}(OH_2)$ and Ru^{II}_{K97C}–$[(P)Fe^{IV}_{P450}(OH)$ (Compound II). The conversion of Ru^{II}_{K97C}–$(P^{\cdot+})Fe^{III}_{P450(A)}(OH_2)$ to Ru^{II}_{K97C}–$[(P^{\cdot+})Fe^{III}_{P450(B)}$ (OH_2) was rationalized by solvent or polypeptide conformational changes, as with MP8 and HRP. The conversion from ferric radical cation Ru^{II}–$[(P^{\cdot+})Fe^{III}(OH_2)$ to ferryl Ru^{II}_{K97C}–$[(P)Fe^{IV}_{P450}(OH)$ is pH dependent, both of which are present transiently and a fast recovery to the initial complex Ru^{II}_{K97C}–Fe^{III}_{P450} is observed [135]. Similarly, Farmer and co-workers [136] reported another example in which the photosensitizer $[Ru(bpy)_3]^{2+}$ was attached covalently to a heme enzyme via a $-(CH_2)_7-$ linker (L62). This linking strategy was already reported by Oishi and co-workers as earlier as 1999, who demonstrated that it facilitated intramolecular electron transfer with observation of the ferric–porphyrin cation radical spectroscopically [137]. In contrast to Ru^{II}_{K97C}–Fe^{III}_{P450}, the distance between photosensitizer and heme unit was large enough to prevent recovery from the ferric porphyrin radical species Ru^{II}–$(P^{\cdot+})Fe^{III}$ to the initial Ru^{II}–Fe^{III} state. The fate of this ferric radical is either to oxidize the iron center to form the ferryl form (Compound II) or oxidize a surrounding amino acid residue (Fig. 13). The oxidation of the protein also suggested that the protein environment significant influenced the reaction [136].

In addition to the photoxidation strategy in Fig. 12b, there is also a photoreductive strategy, in which the electron acceptor ($[Ru(NH_3)_6]^{3+}$, $[Co(NH_3)_5Cl]^{2+}$) is replaced by electron donor (e.g., diethyldithiocarbamate = DTC). As an excitation quencher DTC, reduces the excited $[Ru(bpy)_3]^{2+*}$ to $[Ru(bpy)_3]^{+}$, which is a strong reductant (−1.26 V vs SCE). As with the modified photooxidative strategy, a polypyridyl Ru(II) moiety was attached covalently to a heme enzyme, however, the fate of the intermediate Ru(I)-Fe(III) species is not as clear as in the photo oxidative strategy. Nevertheless, C—H functionalization studies show higher total turnover numbers under irradiation with visible light than control reactions [138], which further emphasizes that reactivity can be controlled both by the varying the nature of photosensitizer and modification of the heme structure [139]. In short, several successful examples to use photochemistry to trigger the reactivity of heme metalloenzymes have been described in this field can expect further development in the near future [140,141]. However, as will be discussed below, these studies may need to be revisited to take into consideration the intrinsic photochemistry of the iron complexes themselves.

3.5.1.2. Photosensitized non-heme based catalytic systems. The number of heme and non-heme iron dependent enzymes involved in oxidations make mimicking such systems highly attractive in biomimetic catalyst design. Several high-valent complexes of bioinorganic relevance have been reported generated with oxidants and there are recently several reports of their photochemical generation. Fukuzumi and co-workers [132] reported the first photochemical generation of a non-heme high-valent iron-oxo

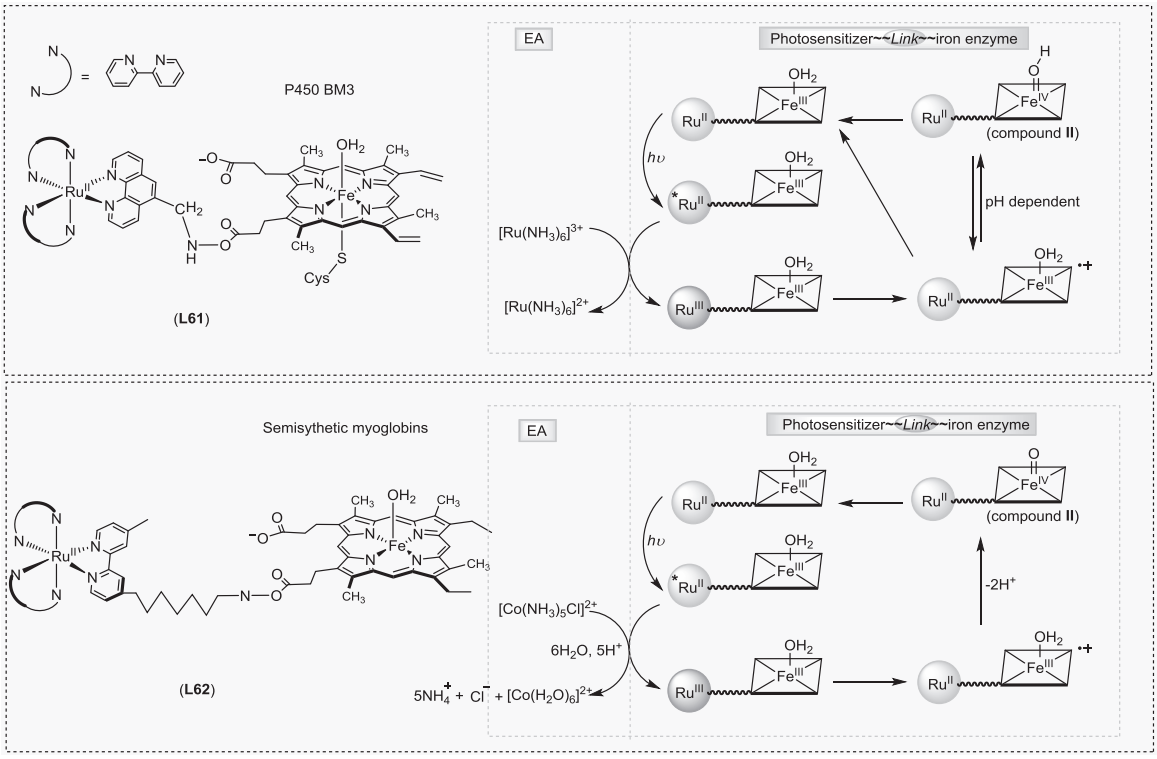

Fig. 14. Examples of generation of high-valent metalloenzymes by a modified multi catalyst strategy.

complex with the pentadentate polypyridyl ligand N4Py (L63) in 2010 using a photo-induced oxidative pathway (Fig. 12b). The photosensitizer $[Ru(bpy)_3]^{2+}$ when excited with visible light is oxidized by the electron acceptor $[Co(NH_3)_5Cl]^{2+}$ to form $[Ru(bpy)_3]^{3+}$, which in turn oxidizes the non-heme Fe^{II} complex (L63) to the Fe^{IV}-=O complex (with water as the oxygen source) in a step-wise manner (Fig. 15) [132].

Later in 2014, Dhar and co-worker [142] reported the first photochemical generation of iron(V)-oxo with tetra-amidomacrocyclic TAML ligands (L64 and L65). In this case, they started with Fe^{III} complex as in heme system, and $S_2O_8^{2-}$ was used as electron acceptor. The Fe^{III} state was oxidized to Fe^{IV}=O state first as $[Ru(bpy)_3]^{3+}$ is not strong enough to oxidize Fe^{IV} state to Fe^{V} state. This step contrasts with the previous case. The formation of Fe^{V} was attributed to the SO_4^{-} radical oxidation (Fig. 15) [142] and this reactive intermediate is responsible for water oxidation. In 2017, the complex L64 was also studied for its photocatalytic hydroxylation and epoxidation reaction by Sen Gupta and co-workers [143]. Notably, in this photocatalytic reaction the SO_4^{-} radical species is not observed due to the use of $[Co(NH_3)_5Cl]^{2+}$ as electron acceptor instead of $S_2O_8^{2-}$. The $(L64)Fe^{IV}$ monomer formed immediately forms the dimer $[\{(L64)Fe^{IV}\}_2(\mu\text{-}O)]^{2+}$, which is the active oxidant [143].

As with heme systems, the covalent linking strategy binding photosensitizer to the iron complex was also used in non-heme systems. Banse and co-workers [144] reported a chromophore-catalyst complex L66 (Fig. 16), in which the non-heme iron complex was attached covalently to the photosensitizer ($[Ru(bpy)_3]^{2+}$) as in the heme systems (L61 and L62). The complex $[Ru^{II}\text{-}Fe^{II}(OH_2)]^{2+}$ was promoted to the excited state $[*Ru^{II}\text{-}Fe^{II}(OH_2)]^{2+}$ under irradiation ($\lambda = 450$ nm), which then formed $[Ru^{III}\text{-}Fe^{II}(OH_2)]^{2+}$ by oxidation with $[Ru(NH_3)_6]^{3+}$, followed by intramolecular electron transfer from iron(II) center to ruthenium(III) center to form $[Ru^{II}\text{-}Fe^{III}(OH)]^{2+}$. The high-valent of $[Ru^{II}\text{-}Fe^{IV}(O)]^{2+}$ complex was formed by a second cycle (Fig. 16) [144].

In addition to the photosensitized oxidative formation of high-valent iron complexes, a photosensitized reductive pathway to form a high-valent iron complex can be used in the catalytic oxidation of PPh_3 with several turnovers [145]. Instead of an electron acceptor, Et_3N was used as an electron donor. The excited state $[Ru(bpy)_3]^{2+*}$ was quenched to form Ru(I) complex $[Ru(bpy)_3]^{+}$ which is a strong reductant (−1.26 V vs SCE) and reduces the diiron(III) complex to mononuclear Fe(II). Subsequent reaction with molecular oxygen to form μ-peroxo diiron(III) complex and then higher oxidation states to form two iron(IV)-oxo moieties that are responsible for substrate oxidation (Fig. 17). Notably, the covalently linked complex L67 shows lower photo-efficiency than the non-covalently connected Ru/iron system, presumably due to deactivation of the ruthenium complexes excited state by deprotonation of the imidazole linker [145]. In this studies dioxygen activation and formation of μ-peroxo diiron(III) complex were demonstrated, however, the formation of iron(IV)=O species was not confirmed.

In summary, in both heme and non-heme systems, the use of photosensitizers dramatically increases the reactivity of the iron complexes/enzyme. Covalent linking of the photosensitizer and iron complex further contributes to efficiency through intramolecular electron transfer. However, as for heme based photosensitized systems, in the non-heme systems there is still an open question as to the impact the photoreactivity of the iron complexes themselves. As is discussed below, these latter systems open opportunities for photo-driven oxidation with a single catalyst.

3.5.2. Photo-catalytic reactions through direct photo-excitation of iron complexes

3.5.2.1. Direct photo activation of mononuclear heme iron complexes. Direct photoactivation of a heme complex was reported by Newcomb and co-workers in 2005 [146]. The photooxidation of Compound **II** (a neutral iron(IV)-oxo porphyrin compound) to Compound **I** (a radical iron(IV)-oxo porphyrin compounds) occurs under UV irradiation ($\lambda = 355$ nm, Fig. 18b), for complexes L68,

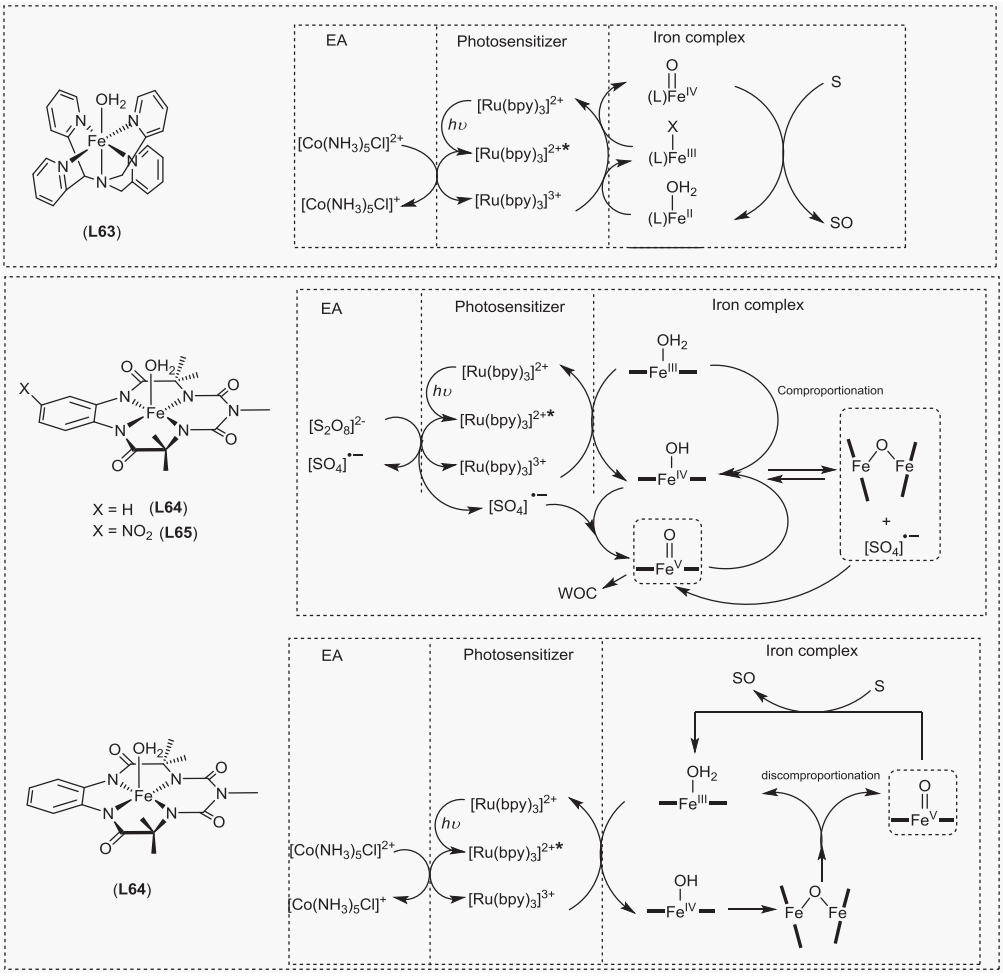

Fig. 15. Examples of the photosensitized catalytic reactions in non-heme systems.

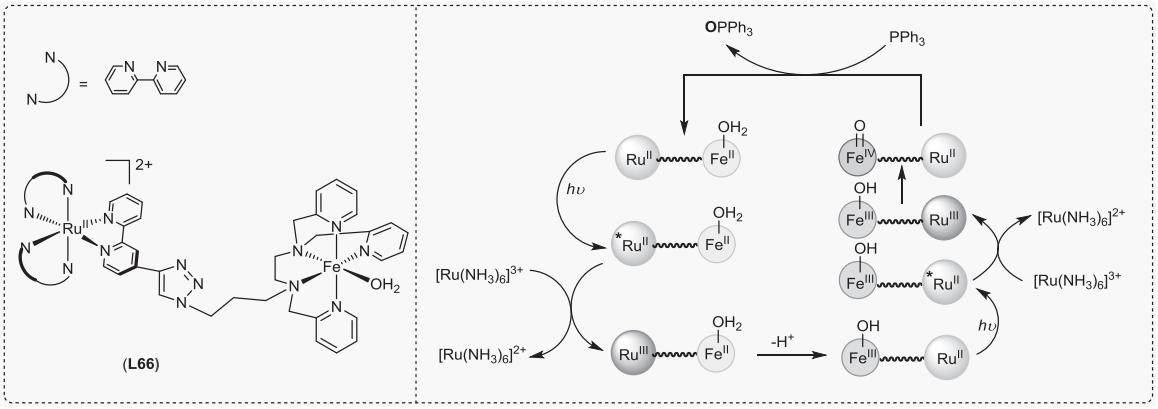

Fig. 16. Examples of the modified photosensitized catalytic reaction in non-heme systems.

horseradish peroxidase (HRP) (L69) and horse skeletal Myoglobin. Usually, compound **I** models are formed by addition of terminal oxidants (H_2O_2, PhIO, m-CPBA) to the porphyrin-iron(III) precursor, followed by reaction with substrates to form the relatively stable compound **II**. Under irradiation, compound **II** forms compound **I**, manifested in a change in UV–vis absorption and compound **I** persists for several seconds in the absence of substrates [146].

Later, the same group reported photochemical generation of even higher oxidation states, i.e. an iron(V)-oxo porphyrin complex (Fig. 18c) [147]. The porphyrin(IV)=O complex has a axial substituent (NO_2, ClO_2), which under UV irradiation ($\lambda = 350$ nm) undergoes heterolytic cleavage to form iron(V)-oxo compounds, which react over 100 times more rapidly with substrates than the corresponding iron(IV) compound [147].

3.5.2.2. The direct photo activation of dinuclear heme iron complexes. The light-driven catalytic oxidation of substrates using a single iron-containing catalyst that can undergo direct photoexcitation

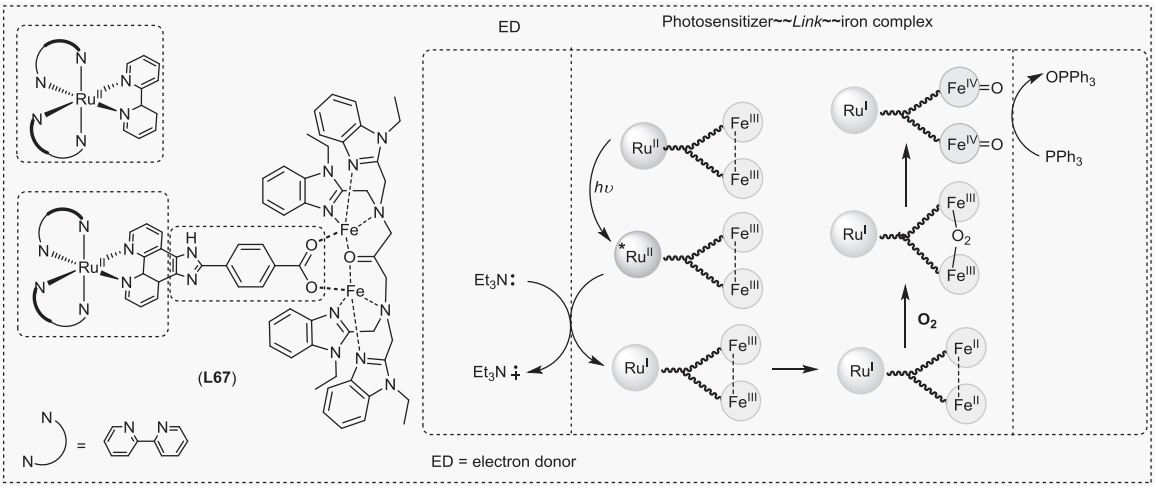

Fig. 17. Examples of photo-induced reductive formation high-valent iron complex.

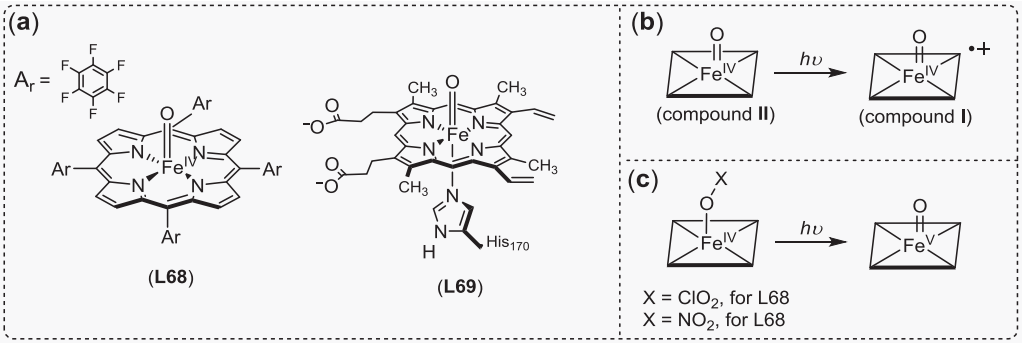

Fig. 18. Examples of photolysis reaction on heme system.

is highly attractive in simplifying the design of catalytic systems. In this regard, photo-induced disproportionation of porphyrin diiron (III) complexes is one of most promising pathways. Richman and co-workers [148] reported the first example of photo-induced hetero-cleavage of the oxo-bridge of a μ-oxo porphyrin diiron(III) $[(FeTPP)_2O]^{4+}$ complex (L70) with formation of 2 equiv. of $Fe^{II}TPP$ as the final product under UV-irradiation (O → Fe LMCT band), accompanied by the oxidation of the substrate PPh_3. The Fe(III)-O-Fe(III) complex was regenerated by oxidation with molecular oxygen. Formation of high-valent iron(IV)-oxo intermediates (Fe^{IV}-OTPP) via disproportionation was proposed based on substrate oxidation patterns, as well as, quantum yields [148,149]. The water soluble complex (L71) showed similar photo-induced disproportionation reactions [150].

Nocera and co-workers [151] reported a strategy for selective oxidation of substrates using μ-oxo porphyrin diiron(III) complexes under photo catalytic conditions. Cofacial bisporphyrine μ-oxo diiron(III) complexes bearing dibenzofuran (DPD, L74) and xanthene (DPX, L75) (Fig. 19), in which the two 'Pacman' moieties were used as a pillar to build up a molecular spring architecture, confined the attack on the substrates to favor a side-on geometry. The size of the two spacers controls the pocket size for the substrates and inhibits recombination to form the μ-oxo diiron(III) states. The photocatalytic oxidation of substrates (dimethyl sulfoxide) was studied and compared with the complex without such a spacer (L72). The DPD-bridged complex L74 shows similar quantum efficiency to the non-bridged complex L72, but much higher efficiency towards substrate oxidation [151,152]. Later, this spring-loaded complex was further modified in the porphyrin ring with three pentafluorophenyl groups (L73), which showed higher turnover numbers towards sulfide [153], olefin [153], and hydrocarbon oxidation [154] under visible light irradiation with molecular oxygen as terminal oxidation and without use of a co-reductant. An ethane linked cofacial diiron(III) μ-oxo porphyrin reported by Rath and co-workers [155] showed photocatalytic oxidation of $P(OR_3)$ (R: Me, Et) via a photo-induced disproportionation reaction mechanism. The pillar linked cofacial diiron(III) μ-oxo porphyrin complexes show a common feature in that they have much smaller Fe-O-Fe angles (150–160°) compared to the 170–178° of non-covalently linked complexes and favor attack on substrates in a side-on manner [155].

The first system with inequivalent ligands (i.e. heme/nonheme) was the μ-oxo diiron(III) [$(L)Fe^{III}$-O-Fe^{III}(L'), L77] complex reported by Karlin and co-workers in 2004 (Fig. 19c) [156], which shows photo-induced catalytic oxidation of a series of substrates, PPh_3 to $OPPh_3$, tetrahydrofuran to γ-butyrolactone, and toluene to benzaldehyde. Transient absorption spectroscopy indicates that the photo-induced disproportionation of the μ-oxo diiron(III) to form an Fe^{IV}=O/Fe^{II} pair occurs, in which the Fe^{IV}=O is the reactive towards substrate oxidation [156]. Notably, photo-induced disproportionation of diiron(III) is not the only case reported, with an even higher oxidation state, iron(V) generated by photo-induced disproportionation of a bis-corrole-diiron(IV)-μ-oxo dimer together with one equiv. iron(III). The reactivity of the iron(V) intermediates is greater than that of the corresponding iron(IV) complex [157].

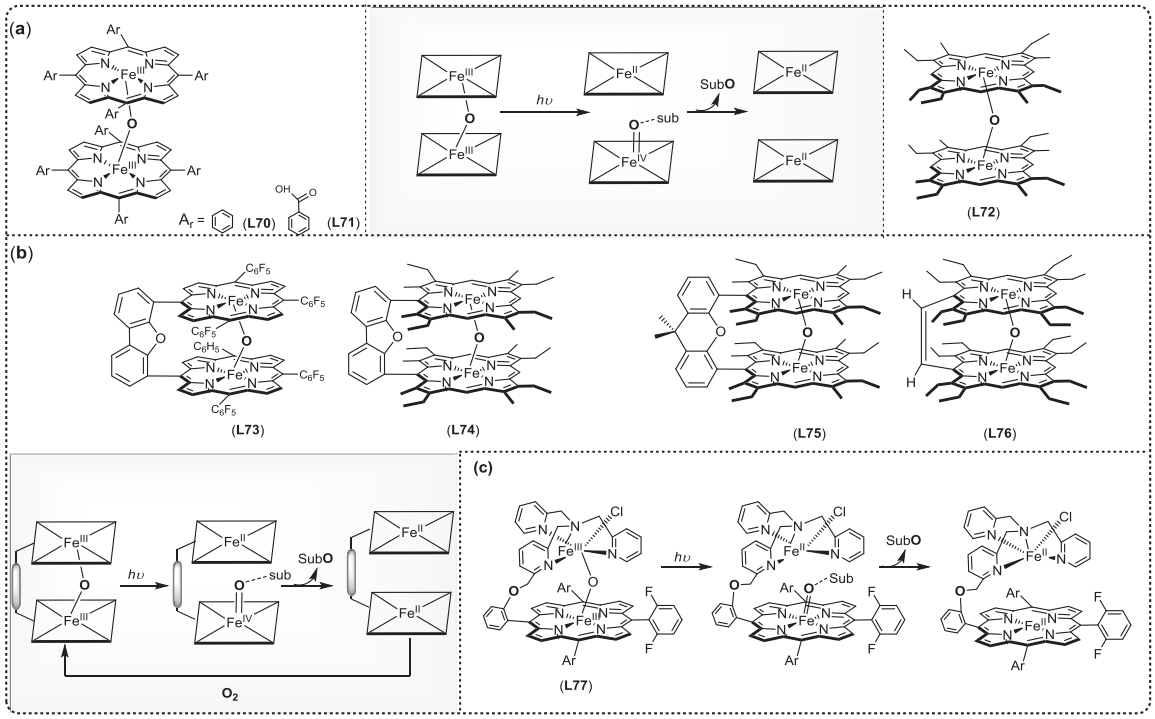

Fig. 19. Examples of photo-induced disproportionation of diiron(III) porphyrin complexes.

Form the discussion above, we can conclude that the photo-induced disproportionation of μ-oxo diiron(III)/diiron(IV) is a promising strategy in photocatalytic oxidations with iron complexes. The intermediate high-valent iron complexes formed are key reactive species. However, limitations remain; the quantum yield in these heme systems is quite low due to the large driving force for recombination of Fe(IV)═O and Fe(II) units, which shuts down productive oxidation pathways. Compared to the heme system, the non-heme iron complex provides greater flexibility in terms of ligand modification. Furthermore the thermal reactivity toward a variety of substrates with non-heme high-valent iron-oxo complexes has been studied extensively. Hence it is worthwhile to explore driving the oxidation of organic substrates by non-heme iron complexes photochemically.

3.5.2.3. The direct photo activation of non heme iron complexes. The potential application of non-heme iron complexes under photochemical conditions requires that they are stable under catalytic conditions (e.g., Fe^{II}, Fe^{III}, and Fe^{IV} in certain cases) and hence Fe^{I} and Fe^{V} complexes, which are highly reactive at ambient conditions, are considered as intermediates only. Although non-heme iron photochemistry is dominated by photo-induced decarboxylation of iron(III) complexes, discussed in Sections 3.1, 3.2, and more recent reports of the photochemistry of iron(II) complexes in relation to the activation of dioxygen (see below), direct activation (as opposed to systems in which a photosensitizer is used) of non-heme iron complexes is not readily apparent from the literature.

The photo-induced oxidation of a non-heme iron(II) complex in the presence of molecular oxygen as the terminal oxidant (L78 and L79 in Fig. 20a) was reported first in 2009 [158]. The non-heme iron(II) complex (L78), designed as a functional mimic of iron bleomycin and studied extensively in its reactivity with oxidants such as H_2O_2, forms reactive high-valent iron-oxo species with certain terminal oxidants [159]. Irradiation of $[(L78)Fe(II)OCH_3]^{2+}$ in aerobic methanol or $[(L78)Fe(II)OH]^{2+}$ in H_2O results in oxidation to the corresponding solvent-coordinated iron(III) complex. Under anaerobic conditions in acetonitrile oxidation does not occur due to the highly favorable coordination of acetonitrile to the Fe^{II} center in acetonitrile. Later, Bartlett and co-workers reported a non-heme iron(II) complex bearing a tetradentate (bpmcn) ligand (L80 in Fig. 20b), which undergoes similar photo-induced oxidation from the iron(II) to iron(III) states by activation of dioxygen. In this case, there are two labile coordination sites on the iron center compared with the one site available in the L78 based complex and hence O_2 coordination is expected to be more facile, and photo-induced oxidation occurs in acetonitrile also [160].

Recently, the effect of near UV-excitation on the reactivity of a series of non-heme iron(IV)-oxo complexes towards C—H activation was reported (Fig. 21) [161]. Hydrogen atom abstraction (HAT) of a C—H bond shows a large kinetic isotope effect (KIE) in the thermal reaction between the Fe(IV)═O species and alkanes, consistent with HAT as the rate-determining step, however, although the reaction is accelerated by photoexcitation the KIE is much reduced ($k_H \approx k_D$). The wavelength dependence of the activation (only near-UV light accelerates the thermal reaction) suggested the excitation into the near-UV ligand(oxo)-to-metal charge-transfer (LMCT). This charger redistribution results in a weakening and hence elongation of the Fe(IV)—O bond and an increase in its oxyl radical character, making it a more powerful C—H bond abstracting agent.

More recently, the photocatalytic oxidation of methanol was reported using a single photo-catalyst, the non-heme iron(III) complexes $[(L)Fe^{III}\text{-}X]^{2+}$ (L = N4Py (L78), MeN4Py (L79); X = Cl, OCH_3, Fig. 22)) [162]. Under anaerobic irradiation in methanol, the non-heme iron(III) complex undergoes photo reduction to form the corresponding $[(L)Fe^{II}\text{-}X]^{2+}$ without ligand degradation, and, more importantly, is accompanied by oxidation of sub stoichiometric methanol to formaldehyde. Mechanistic studies indicate the most likely reactive species is its corresponding μ-oxo-dimer, an Fe^{III}-μ-O-Fe^{III} complex, which is formed and in equilibrium with monomer ($[(L)Fe^{III}\text{-}X]^{2+}$) complex upon dissolution in methanol, the dinuclear complex undergoes photo-induced disproportionation to form $[(L)Fe^{II}\text{-}X]^{2+}$ and $[(L)Fe^{IV}{=}O]^{2+}$ species, and it is the high-valent iron(IV)-oxo that is responsible for methanol

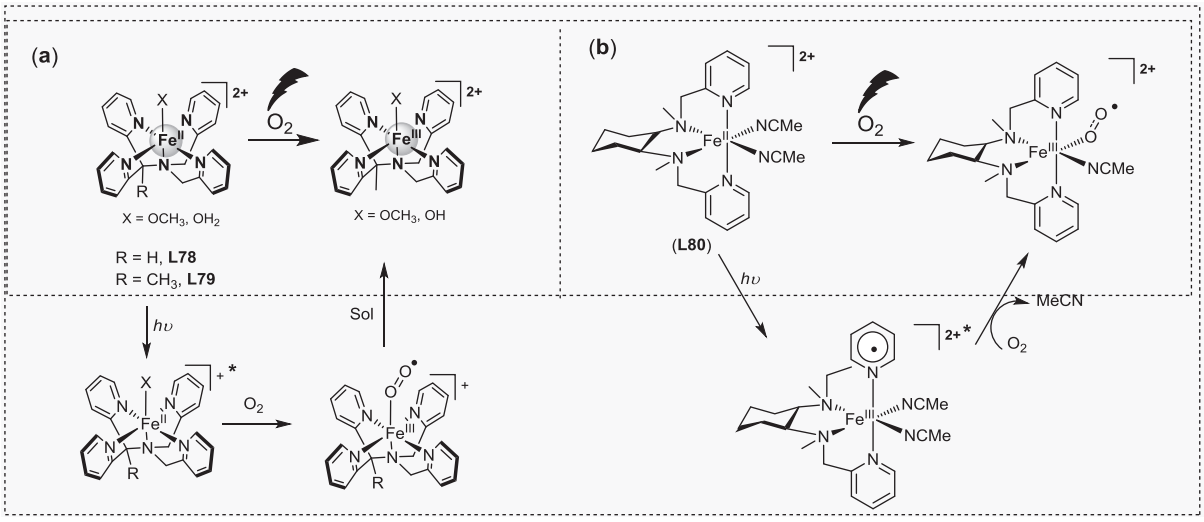

Fig. 20. Examples of photo-induced oxidation of non-heme iron(II) complexes with molecular oxygen as terminal oxidant.

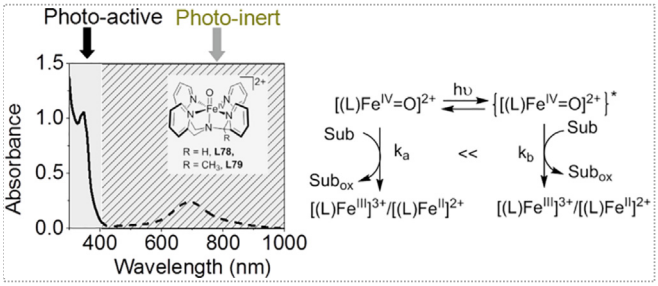

Fig. 21. Direct photochemical activation of non-heme Fe(IV)=O complexes.

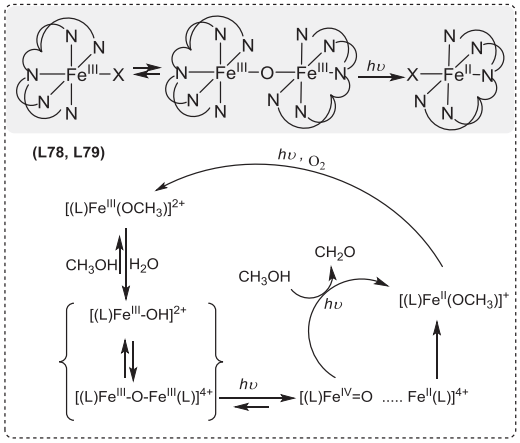

Fig. 22. A non-heme iron photo-catalyst for light driven aerobic oxidation of methanol.

oxidation. The reactivity is further enhanced by excitation of the iron(IV)=O at same wavelength (vide supra). This mechanism was supported by the transient observation of the high-valent iron(IV)-oxo species upon irradiation into the LMCT band of the Fe^{III}-μ-O-Fe^{III} complex at high concentrations. Together with the previous report of photooxidation (from $[(L)Fe^{II}\text{-}X]^{+}$ to $[(L)Fe^{III}\text{-}X]^{2+}$) with molecular oxygen as terminal oxidant, the photocatalytic cycle (methanol oxidation to methanal with O_2) is closed, and high turnover numbers were obtained by irradiation of $[(L)Fe^{III}\text{-}X]^{2+}$ as a single (photo)catalyst in aerobic methanol with only minor catalyst deactivation over time [163].

4. Conclusion and overview

The photochemistry of iron complexes continues to surprise and it is clear that the paradigm that iron complexes show limited photochemistry due to the rapid excited state relaxation that occurs via low-lying metal centered states of iron complexes is increasingly challenged. The possibility of activating iron complexes in a range of oxidation states towards oxidative transformations opened opportunities in photoredox catalysis. However, whereas the heme systems are amenable to study by time resolved spectroscopies, probing the excited states responsible for the photochemical reactions in non-heme iron complexes remains a challenge to be met.

Acknowledgments

Financial support was provided by The Netherlands Ministry of Education, Culture and Science (Gravity Program 024.001.035 to W.R.B.) and Chinese Scholarship Council (J.C.). COST action CM1305 ECOSTBio is acknowledged for discussion.

Appendix A. Supplementary data

Supplementary data associated with this article can be found, in the online version, at https://doi.org/10.1016/j.ccr.2018.06.008.

References

[1] T. van Leeuwen, A.S. Lubbe, P. Štacko, S.J. Wezenberg, B.L. Feringa, Dynamic control of function by light-driven molecular motors, Nat. Rev. Chem. 1 (2017) 96, https://doi.org/10.1038/s41570-017-0096.
[2] E.C. Harvey, B.L. Feringa, J.G. Vos, W.R. Browne, M.T. Pryce, Transition metal functionalized photo- and redox-switchable diarylethene based molecular switches, Coord. Chem. Rev. 282–283 (2015) 77–86, https://doi.org/10.1016/j.ccr.2014.06.008.
[3] B. Vincenzo, C. Alberto, V. Margherita, Photochemical conversion of solar energy, ChemSusChem 1 (2008) 26–58, https://doi.org/10.1002/cssc.200700087.
[4] P. Agostinis, K. Berg, K.A. Cengel, T.H. Foster, A.W. Girotti, S.O. Gollnick, S.M. Hahn, M.R. Hamblin, A. Juzeniene, D. Kessel, M. Korbelik, J. Moan, P. Mroz, D. Nowis, J. Piette, B.C. Wilson, J. Golab, Photodynamic therapy of cancer: an update, CA, Cancer J. Clin. 61 (2011) 250–281, https://doi.org/10.3322/caac.20114.
[5] R.M.N. Yerga, M.C.Á. Galván, F. del Valle, J.A. Villoria de la Mano, J.L.G. Fierro, Water splitting on semiconductor catalysts under visible-light irradiation, ChemSusChem 2 (2009) 471–485, https://doi.org/10.1002/cssc.200900018.
[6] V. Balzani, G. Bergamini, S. Campagna, F. Puntoriero, Photochemistry and photophysics of coordination compounds: overview and general concepts BT

– photochemistry and photophysics of coordination compounds I, Springer Berlin Heidelberg, Berlin, Heidelberg, 2007, pp. 1–36, https://doi.org/10.1007/128_2007_132.
[7] S. Campagna, F. Puntoriero, F. Nastasi, G. Bergamini, V. Balzani, Photochemistry and photophysics of coordination compounds: ruthenium BT – photochemistry and photophysics of coordination compounds I, Springer Berlin Heidelberg, Berlin, Heidelberg, 2007, pp. 117–214, https://doi.org/10.1007/128_2007_133.
[8] N.A.P. Kane-Maguire, Photochemistry and photophysics of coordination compounds: chromium BT – photochemistry and photophysics of coordination compounds I, Springer Berlin Heidelberg, Berlin, Heidelberg, 2007, pp. 37–67, https://doi.org/10.1007/128_2007_141.
[9] S. Ye, C. Kupper, S. Meyer, E. Andris, R. Navrátil, O. Krahe, B. Mondal, M. Atanasov, E. Bill, J. Roithová, F. Meyer, F. Neese, Magnetic circular dichroism evidence for an unusual electronic structure of a tetracarbene–oxoiron(IV) complex, J. Am. Chem. Soc. 138 (2016) 14312–14325, https://doi.org/10.1021/jacs.6b07708.
[10] K.-B. Cho, H. Hirao, S. Shaik, W. Nam, To rebound or dissociate? This is the mechanistic question in C-H hydroxylation by heme and nonheme metal-oxo complexes, Chem. Soc. Rev. 45 (2016) 1197–1210, https://doi.org/10.1039/C5CS00566C.
[11] A.R. McDonald, L. Que, High-valent nonheme iron-oxo complexes: synthesis, structure, and spectroscopy, Coord. Chem. Rev. 257 (2013) 414–428, https://doi.org/10.1016/j.ccr.2012.08.002.
[12] J. England, Y. Guo, K.M. Van Heuvelen, M.A. Cranswick, G.T. Rohde, E.L. Bominaar, E. Münck, L. Que, A More Reactive Trigonal-Bipyramidal High-Spin Oxoiron(IV) Complex with a cis-Labile Site, J. Am. Chem. Soc. 133 (2011) 11880–11883, https://doi.org/10.1021/ja2040909.
[13] J. England, M. Martinho, E.R. Farquhar, J.R. Frisch, E.L. Bominaar, E. Münck, L. Que, A synthetic high-spin oxoiron(IV) complex: generation, spectroscopic characterization, and reactivity, Angew. Chem. Int. Ed. 48 (2009) 3622–3626, https://doi.org/10.1002/anie.200900863.
[14] A.N. Biswas, M. Puri, K.K. Meier, W.N. Oloo, G.T. Rohde, E.L. Bominaar, E. Münck, L. Que, Modeling TauD-J: A High-Spin Nonheme Oxoiron(IV) Complex with High Reactivity toward C-H Bonds, J. Am. Chem. Soc. 137 (2015) 2428–2431, https://doi.org/10.1021/ja511757j.
[15] A. Juris, V. Balzani, F. Barigelletti, S. Campagna, P. Belser, A. von Zelewsky, Ru (II) polypyridine complexes: photophysics, photochemistry, eletrochemistry, and chemiluminescence, Coord. Chem. Rev. 84 (1988) 85–277, https://doi.org/10.1016/0010-8545(88)80032-8.
[16] P. Chábera, Y. Liu, O. Prakash, E. Thyrhaug, A. El Nahhas, A. Honarfar, S. Essén, L.A. Fredin, T.C.B. Harlang, K.S. Kjær, K. Handrup, F. Ericson, H. Tatsuno, K. Morgan, J. Schnadt, L. Häggström, T. Ericsson, A. Sobkowiak, S. Lidin, P. Huang, S. Styring, J. Uhlig, J. Bendix, R. Lomoth, V. Sundström, P. Persson, K. Wärnmark, A low-spin Fe(iii) complex with 100-ps ligand-to-metal charge transfer photoluminescence, Nature 543 (2017) 695, https://doi.org/10.1038/nature21430.
[17] D. Patra, A.H. Chaaban, S. Darwish, H.A. Saad, A.S. Nehme, T.H. Ghaddar, Time resolved study of three ruthenium(II) complexes at micellar surfaces: A new long excited state lifetime probe for determining critical micelle concentration of surfactant nano-aggregates, Colloids Surfaces B Biointerfaces 138 (2016) 32–40, https://doi.org/10.1016/j.colsurfb.2015.11.037.
[18] J. Van Houten, R.J. Watts, Effect of ligand and solvent deuteration on the excited state properties of the tris(2,2′-bipyridyl)ruthenium(II) ion in aqueous solution. Evidence for electron transfer to solvent, J. Am. Chem. Soc. 97 (1975) 3843–3844, https://doi.org/10.1021/ja00846a062.
[19] W. Gawelda, A. Cannizzo, V.-T. Pham, F. van Mourik, C. Bressler, M. Chergui, Ultrafast nonadiabatic dynamics of [FeII(bpy)3]2+ in solution, J. Am. Chem. Soc. 129 (2007) 8199–8206, https://doi.org/10.1021/ja070454x.
[20] Y. Liu, T. Harlang, S.E. Canton, P. Chabera, K. Suarez-Alcantara, A. Fleckhaus, D. A. Vithanage, E. Goransson, A. Corani, R. Lomoth, V. Sundstrom, K. Warnmark, Towards longer-lived metal-to-ligand charge transfer states of iron(ii) complexes: an N-heterocyclic carbene approach, Chem. Commun. 49 (2013) 6412–6414, https://doi.org/10.1039/C3CC43833C.
[21] Y. Liu, P. Persson, V. Sundström, K. Wärnmark, Fe N-heterocyclic carbene complexes as promising photosensitizers, Acc. Chem. Res. 49 (2016) 1477–1485, https://doi.org/10.1021/acs.accounts.6b00186.
[22] C. Brady, P.L. Callaghan, Z. Ciunik, C.G. Coates, A. Døssing, A. Hazell, J.J. McGarvey, S. Schenker, H. Toftlund, A.X. Trautwein, H. Winkler, J.A. Wolny, Molecular structure and vibrational spectra of spin-crossover complexes in solution and colloidal media: resonance Raman and time-resolved resonance Raman studies, Inorg. Chem. 43 (2004) 4289–4299, https://doi.org/10.1021/ic049809t.
[23] J. Kiwi, C. Pulgarin, P. Peringer, M. Grätzel, Beneficial effects of homogeneous photo-Fenton pretreatment upon the biodegradation of anthraquinone sulfonate in waste water treatment, Appl. Catal. B Environ. 3 (1993) 85–99, https://doi.org/10.1016/0926-3373(93)80070-T.
[24] H.J.H. Fenton, LXXIII.-Oxidation of tartaric acid in presence of iron, J. Chem. Soc. Trans. 65 (1894) 899–910, https://doi.org/10.1039/CT8946500899.
[25] J.J. Pignatello, Dark and photoassisted iron(3+)-catalyzed degradation of chlorophenoxy herbicides by hydrogen peroxide, Environ. Sci. Technol. 26 (1992) 944–951, https://doi.org/10.1021/es00029a012.
[26] S.H. Bossmann, E. Oliveros, S. Göb, S. Siegwart, E.P. Dahlen, L. Payawan, M. Straub, M. Wörner, A.M. Braun, New evidence against hydroxyl radicals as reactive intermediates in the thermal and photochemically enhanced fenton reactions, J. Phys. Chem. A 102 (1998) 5542–5550, https://doi.org/10.1021/jp980129j.
[27] F. Harber, J. Weiss, The catalytic decomposition of hydrogen peroxide by iron salts, Proc. R. Soc. London. Ser. A – Math. Phys. Sci. 147 (1934) 332–351, http://rspa.royalsocietypublishing.org/content/147/861/332.abstract.
[28] M. Barbeni, C. Minero, E. Pelizzetti, E. Borgarello, N. Serpone, Chemical degradation of chlorophenols with Fenton's reagent (Fe2+ + H2O2), Chemosphere 16 (1987) 2225–2237, https://doi.org/10.1016/0045-6535(87)90281-5.
[29] L. Cermenati, P. Pichat, C. Guillard, A. Albini, Probing the TiO2 photocatalytic mechanisms in water purification by use of quinoline, photo-fenton generated OH• radicals and superoxide dismutase, J. Phys. Chem. B 101 (1997) 2650–2658, https://doi.org/10.1021/jp962700p.
[30] C. Domínguez, J. García, M.A. Pedraz, A. Torres, M.A. Galán, Photocatalytic oxidation of organic pollutants in water, Catal. Today 40 (1998) 85–101, https://doi.org/10.1016/S0920-5861(97)00125-9.
[31] P. Borer, S.J. Hug, Photo-redox reactions of dicarboxylates and α-hydroxydicarboxylates at the surface of Fe(III)(hydr)oxides followed with in situ ATR-FTIR spectroscopy, J. Colloid Interface Sci. 416 (2014) 44–53, https://doi.org/10.1016/j.jcis.2013.10.030.
[32] C. Weller, S. Horn, H. Herrmann, Photolysis of Fe(III) carboxylato complexes: Fe(II) quantum yields and reaction mechanisms, J. Photochem. Photobiol. A Chem. 268 (2013) 24–36, https://doi.org/10.1016/j.jphotochem.2013.06.022.
[33] J. Šima, J. Makáňová, Photochemistry of iron (III) complexes, Coord. Chem. Rev. 160 (1997) 161–189, https://doi.org/10.1016/S0010-8545(96)01321-5.
[34] I.P. Pozdnyakov, F. Wu, A.A. Melnikov, V.P. Grivin, N.M. Bazhin, S.V. Chekalin, V.F. Plyusnin, Photochemistry of iron(iii)-lactic acid complex in aqueous solutions, Russ. Chem. Bull. 62 (2013) 1579–1585, https://doi.org/10.1007/s11172-013-0227-6.
[35] A new sensitive chemical actinometer. I. Some trials with potassium ferrioxalate, Proc. R. Soc. London. Ser. A. Math. Phys. Sci. 220 (1953) 104 LP-116. http://rspa.royalsocietypublishing.org/content/220/1140/104.abstract.
[36] Z. Wang, X. Chen, H. Ji, W. Ma, C. Chen, J. Zhao, Photochemical cycling of iron mediated by dicarboxylates: special effect of malonate, Environ. Sci. Technol. 44 (2010) 263–268, https://doi.org/10.1021/es901956x.
[37] A new sensitive chemical actinometer – II. Potassium ferrioxalate as a standard chemical actinometer, Proc. R. Soc. London. Ser. A. Math. Phys. Sci. 235 (1956) 518–536. http://rspa.royalsocietypublishing.org/content/235/1203/518.abstract.
[38] D.M. Mangiante, R.D. Schaller, P. Zarzycki, J.F. Banfield, B. Gilbert, Mechanism of ferric oxalate photolysis, ACS Earth Sp. Chem. 1 (2017) 270–276, https://doi.org/10.1021/acsearthspacechem.7b00026.
[39] J. Chen, H. Zhang, I.V. Tomov, M. Wolfsberg, X. Ding, P.M. Rentzepis, Transient structures and kinetics of the ferrioxalate redox reaction studied by time-resolved EXAFS, optical spectroscopy, and DFT, J. Phys. Chem. A 111 (2007) 9326–9335, https://doi.org/10.1021/jp0733466.
[40] J. Chen, H. Zhang, I.V. Tomov, P.M. Rentzepis, Electron transfer mechanism and photochemistry of ferrioxalate induced by excitation in the charge transfer band, Inorg. Chem. 47 (2008) 2024–2032, https://doi.org/10.1021/ic7016566.
[41] J. Chen, A.S. Dvornikov, P.M. Rentzepis, Comment on "New insight into photochemistry of ferrioxalate", J. Phys. Chem. A 113 (2009) 8818–8819, https://doi.org/10.1021/jp809535q.
[42] I.P. Pozdnyakov, O.V. Kel, V.F. Plyusnin, V.P. Grivin, N.M. Bazhin, Reply to "Comment on 'New insight into Photochemistry of Ferrioxalate'", J. Phys. Chem. A 113 (2009) 8820–8822, https://doi.org/10.1021/jp810301g.
[43] Z. Wang, C. Chen, W. Ma, J. Zhao, Photochemical coupling of iron redox reactions and transformation of low-molecular-weight organic matter, J. Phys. Chem. Lett. 3 (2012) 2044–2051, https://doi.org/10.1021/jz3005333.
[44] D.A. Thomas, M.M. Coggon, H. Lignell, K.A. Schilling, X. Zhang, R.H. Schwantes, R.C. Flagan, J.H. Seinfeld, J.L. Beauchamp, Real-time studies of iron oxalate-mediated oxidation of glycolaldehyde as a model for photochemical aging of aqueous tropospheric aerosols, Environ. Sci. Technol. 50 (2016) 12241–12249, https://doi.org/10.1021/acs.est.6b03588.
[45] M. Passananti, V. Vinatier, A.-M. Delort, G. Mailhot, M. Brigante, Siderophores in cloud waters and potential impact on atmospheric chemistry: photoreactivity of iron complexes under sun-simulated conditions, Environ. Sci. Technol. 50 (2016) 9324–9332, https://doi.org/10.1021/acs.est.6b02338.
[46] D. Nansheng, W. Feng, L. Fan, X. Mei, Ferric citrate-induced photodegradation of dyes in aqueous solutions, Chemosphere 36 (1998) 3101–3112, https://doi.org/10.1016/S0045-6535(98)00014-9.
[47] J.E. Vernia, M.R. Warmin, J.A. Krause, D.L. Tierney, M.J. Baldwin, Photochemistry and anion-controlled structure of Fe(III) complexes with an α-hydroxy acid-containing tripodal amine chelate, Inorg. Chem. 56 (2017) 13029–13034, https://doi.org/10.1021/acs.inorgchem.7b01799.
[48] K. Barbeau, G. Zhang, D.H. Live, A. Butler, Petrobactin, a photoreactive siderophore produced by the oil-degrading marine bacterium marinobacter hydrocarbonoclasticus, J. Am. Chem. Soc. 124 (2002) 378–379, https://doi.org/10.1021/ja0119088.

[49] F.C. Küpper, C.J. Carrano, J.-U. Kuhn, A. Butler, Photoreactivity of iron(III)–aerobactin: photoproduct structure and iron(III) coordination, Inorg. Chem. 45 (2006) 6028–6033, https://doi.org/10.1021/ic0604967.

[50] J.E. Grabo, M.A. Chrisman, L.M. Webb, M.J. Baldwin, Photochemical reactivity of the iron(III) complex of a mixed-donor, α-hydroxy acid-containing chelate and its biological relevance to photoactive marine siderophores, Inorg. Chem. 53 (2014) 5781–5787, https://doi.org/10.1021/ic500635q.

[51] R.P. Narayanan, G. Melman, N.J. Letourneau, N.L. Mendelson, A. Melman, Photodegradable iron(III) cross-linked alginate gels, Biomacromolecules 13 (2012) 2465–2471, https://doi.org/10.1021/bm300707a.

[52] G.E. Giammanco, C.T. Sosnofsky, A.D. Ostrowski, Light-responsive iron(III)–polysaccharide coordination hydrogels for controlled delivery, ACS Appl. Mater. Interfaces 7 (2015) 3068–3076, https://doi.org/10.1021/am506772x.

[53] V.A. Kumar, N.L. Taylor, A.A. Jalan, L.K. Hwang, B.K. Wang, J.D. Hartgerink, A nanostructured synthetic collagen mimic for hemostasis, Biomacromolecules 15 (2014) 1484–1490, https://doi.org/10.1021/bm500091e.

[54] G.E. Giammanco, B. Carrion, R.M. Coleman, A.D. Ostrowski, Photoresponsive polysaccharide-based hydrogels with tunable mechanical properties for cartilage tissue engineering, ACS Appl. Mater. Interfaces 8 (2016) 14423–14429, https://doi.org/10.1021/acsami.6b03834.

[55] X. Yang, Y. Guo, X. Luo, N. Zheng, T. Ma, J. Tan, C. Li, Q. Zhang, J. Gu, Self-healing, recoverable epoxy elastomers and their composites with desirable thermal conductivities by incorporating BN fillers via in-situ polymerization, Compos. Sci. Technol. 164 (2018) 59–64, https://doi.org/10.1016/j.compscitech.2018.05.038.

[56] W.D. Wagner, K. Nakamoto, Resonance Raman spectra of nitridoiron(V) porphyrin intermediates produced by laser photolysis, J. Am. Chem. Soc. 111 (1989) 1590–1598, https://doi.org/10.1021/ja00187a010.

[57] J. Rittle, M.T. Green, Cytochrome P450 Compound I: Capture, Characterization, and C-H Bond Activation Kinetics, Science 330 (2010) 933–937. http://science.sciencemag.org/content/330/6006/933.abstract.

[58] K. Meyer, E. Bill, B. Mienert, T. Weyhermüller, K. Wieghardt, Photolysis of cis- and trans-[FeIII(cyclam)(N3)2]+ complexes: spectroscopic characterization of a nitridoiron(V) species, J. Am. Chem. Soc. 121 (1999) 4859–4876, https://doi.org/10.1021/ja983454t.

[59] J. Torres-Alacan, J. Lindner, P. Vöhringer, Probing the primary photochemical processes of octahedral iron(V) formation with femtosecond mid-infrared spectroscopy, ChemPhysChem 16 (2015) 2289–2293, https://doi.org/10.1002/cphc.201500370.

[60] J. Torres-Alacan, O. Krahe, A.C. Filippou, F. Neese, D. Schwarzer, P. Vöhringer, The Photochemistry of [FeIIIN3(cyclam-ac)]PF6 at 266 nm, Chem. – A Eur. J. 18 (2012) 3043–3055, https://doi.org/10.1002/chem.201103294.

[61] J. Torres-Alacan, P. Vöhringer, Generating high-valent iron with light: photochemical dynamics from femtoseconds to seconds, Int. Rev. Phys. Chem. 33 (2014) 521–553, https://doi.org/10.1080/0144235X.2014.973197.

[62] J. Torres-Alacan, U. Das, A.C. Filippou, P. Vöhringer, Observing the formation and the reactivity of an octahedral iron(V) nitrido complex in real time, Angew. Chem. Int. Ed. 52 (2013) 12833–12837, https://doi.org/10.1002/anie.201306621.

[63] J.F. Berry, E. Bill, E. Bothe, S.D. George, B. Mienert, F. Neese, K. Wieghardt, An octahedral coordination complex of iron(VI), Science 312 (1937) (2006), LP-1941. http://science.sciencemag.org/content/312/5782/1937.abstract.

[64] T. Petrenko, S. DeBeer George, N. Aliaga-Alcalde, E. Bill, B. Mienert, Y. Xiao, Y. Guo, W. Sturhahn, S.P. Cramer, K. Wieghardt, F. Neese, Characterization of a genuine iron(V)–nitrido species by nuclear resonant vibrational spectroscopy coupled to density functional calculations, J. Am. Chem. Soc. 129 (2007) 11053–11060, https://doi.org/10.1021/ja070792y.

[65] G. Sabenya, L. Lázaro, I. Gamba, V. Martin-Diaconescu, E. Andris, T. Weyhermüller, F. Neese, J. Roithova, E. Bill, J. Lloret-Fillol, M. Costas, Generation, spectroscopic, and chemical characterization of an octahedral iron(V)-nitrido species with a neutral ligand platform, J. Am. Chem. Soc. 139 (2017) 9168–9177, https://doi.org/10.1021/jacs.7b00429.

[66] E. Andris, R. Navrátil, J. Jašík, G. Sabenya, M. Costas, M. Srnec, J. Roithová, Detection of indistinct Fe–N stretching bands in iron(V) nitrides by photodissociation spectroscopy, Chem. – A Eur. J. (2018), https://doi.org/10.1002/chem.201705307.

[67] T. Sjostrand, Endogenous formation of carbon monoxide in man, Nature 164 (1949) 580, https://doi.org/10.1038/164580a0.

[68] E.M. Sikorski, T. Hock, N. Hill-Kapturczak, A. Agarwal, The story so far: molecular regulation of the heme oxygenase-1 gene in renal injury, Am. J. Physiol. Physiol. 286 (2004) F425–F441, https://doi.org/10.1152/ajprenal.00297.2003.

[69] S.W. Ryter, J. Alam, A.M.K. Choi, Heme oxygenase-1/carbon monoxide: from basic science to therapeutic applications, Physiol. Rev. 86 (2006) 583–650, https://doi.org/10.1152/physrev.00011.2005.

[70] B. Widdop, Analysis of carbon monoxide, Ann. Clin. Biochem. 39 (2002) 378–391, https://doi.org/10.1258/000456302760042146.

[71] Y. Gong, T. Zhang, H. Liu, Y. Zheng, N. Li, Q. Zhao, Y. Chen, B. Liu, Synthesis, toxicities and cell proliferation inhibition of CO-releasing molecules containing cobalt, Transit. Met. Chem. 40 (2015) 413–426, https://doi.org/10.1007/s11243-015-9931-4.

[72] S.H. Heinemann, T. Hoshi, M. Westerhausen, A. Schiller, Carbon monoxide - physiology, detection and controlled release, Chem. Commun. 50 (2014) 3644–3660, https://doi.org/10.1039/C3CC49196J.

[73] C.C. Romão, H.L.A. Vieira, Metal carbonyl prodrugs: CO delivery and beyond, in: Bioorganometallic Chem., Wiley-VCH Verlag GmbH & Co. KGaA, 2014, pp. 165–202, https://doi.org/10.1002/9783527673438.ch06.

[74] P.V. Simpson, U. Schatzschneider, Small signaling molecules and CO-releasing molecules (CORMs) for the modulation of the cellular redox metabolism BT – redox-active therapeutics, Springer International Publishing, Cham, 2016, pp. 311–334, https://doi.org/10.1007/978-3-319-30705-3_13.

[75] R. Motterlini, J.E. Clark, R. Foresti, P. Sarathchandra, B.E. Mann, C.J. Green, Carbon monoxide-releasing molecules, Circ. Res. 90 (2002), e17 LP-e24. http://circres.ahajournals.org/content/90/2/e17.abstract.

[76] E. Kottelat, Z. Fabio, Visible light-activated PhotoCORMs, Inorganics 5 (2017), https://doi.org/10.3390/inorganics5020024.

[77] R. Fields, M.M. Germain, R.N. Haszeldine, P.W. Wiggans, Metal carbonyl chemistry. Part IX. Improved syntheses and some reactions of tetracarbonylcyclo-octafluorotetramethyleneiron, J. Chem. Soc. A Inorg. Phys. Theor. (1970) 1964–1969, https://doi.org/10.1039/J19700001964.

[78] R. Victor, R. Ben-Shoshan, S. Sarel, Ferraindene-iron tricarbonyl complexes by a novel dehydrobromination of o-bromostyrene on photolysis with Fe(CO)5, J. Chem. Soc. D Chem. Commun. (1971) 1241–1242, https://doi.org/10.1039/C29710001241.

[79] P. Portius, J. Yang, X.-Z. Sun, D.C. Grills, P. Matousek, A.W. Parker, M. Towrie, M.W. George, Unraveling the photochemistry of Fe(CO)5 in solution: observation of Fe(CO)3 and the conversion between 3Fe(CO)4 and 1Fe(CO)4 (Solvent), J. Am. Chem. Soc. 126 (2004) 10713–10720, https://doi.org/10.1021/ja048411t.

[80] M. Poliakoff, J.J. Turner, Infrared spectra and photochemistry of the complex pentacarbonyliron in solid matrices at 4 and 20 K: evidence for formation of the complex tetracarbonyliron, J. Chem. Soc. Dalton Trans. (1973) 1351–1357, https://doi.org/10.1039/DT9730001351.

[81] M. Poliakoff, J.J. Turner, Structure and reactions of matrix-isolated tetracarbonyliron(0), J. Chem. Soc. Dalton Trans. (1974) 2276–2285, https://doi.org/10.1039/DT9740002276.

[82] M. Poliakoff, Infrared spectrum of matrix isolated tricarbonyliron, J. Chem. Soc. Dalton Trans. (1974) 210–212, https://doi.org/10.1039/DT9740000210.

[83] T.J. Barton, R. Grinter, A.J. Thomson, B. Davies, M. Poliakoff, Magnetic circular dichroism evidence for the paramagnetism of tetracarbonyliron(0): low-temperature matrix studies, J. Chem. Soc. Chem. Commun. (1977) 841–842, https://doi.org/10.1039/C39770000841.

[84] A.J. Atkin, I.J.S. Fairlamb, J.S. Ward, J.M. Lynam, CO release from norbornadiene iron(0) tricarbonyl complexes: importance of ligand dissociation, Organometallics 31 (2012) 5894–5902, https://doi.org/10.1021/om300419w.

[85] R. Kretschmer, G. Gessner, H. Görls, S.H. Heinemann, M. Westerhausen, Dicarbonyl-bis(cysteamine)iron(II): a light induced carbon monoxide releasing molecule based on iron (CORM-S1), J. Inorg. Biochem. 105 (2011) 6–9, https://doi.org/10.1016/j.jinorgbio.2010.10.006.

[86] M.W.W. Adams, The structure and mechanism of iron-hydrogenases, Biochim. Biophys. Acta – Bioenerg. 1020 (1990) 115–145, https://doi.org/10.1016/0005-2728(90)90044-5.

[87] J.W. Tye, M.Y. Darensbourg, M.B. Hall, De novo design of synthetic di-iron(I) complexes as structural models of the reduced form of iron–iron hydrogenase, Inorg. Chem. 45 (2006) 1552–1559, https://doi.org/10.1021/ic051231f.

[88] J. Brown-McDonald, S. Berg, M. Peralto, C. Works, Photochemical studies of iron-only hydrogenase model compounds, Inorganica Chim. Acta 362 (2009) 318–324, https://doi.org/10.1016/j.ica.2008.03.110.

[89] J. Marhenke, A.E. Pierri, M. Lomotan, P.L. Damon, P.C. Ford, C. Works, Flash and continuous photolysis kinetic studies of the iron-iron hydrogenase model (μ-pdt)[Fe(CO)3]2 in different solvents, Inorg. Chem. 50 (2011) 11850–11852, https://doi.org/10.1021/ic201523r.

[90] H.T. Poh, B.T. Sim, T.S. Chwee, W.K. Leong, W.Y. Fan, The dithiolate-bridged diiron hexacarbonyl complex Na2[(μ-SCH2CH2COO)Fe(CO)3]2 as a water-soluble PhotoCORM, Organometallics 33 (2014) 959–963, https://doi.org/10.1021/om401013a.

[91] W.A. Thornley, T.E. Bitterwolf, Intramolecular C. H activation and metallacycle aromaticity in the photochemistry of [FeFe]-hydrogenase model compounds in low-temperature frozen matrices, Chem. – A Eur. J. 21 (2015) 18218–18229, https://doi.org/10.1002/chem.201503826.

[92] X. Jiang, L. Long, H. Wang, L. Chen, X. Liu, Diiron hexacarbonyl complexes as potential CO-RMs: CO-releasing initiated by a substitution reaction with cysteamine and structural correlation to the bridging linkage, Dalton Trans. 43 (2014) 9968–9975, https://doi.org/10.1039/C3DT53620C.

[93] C.S. Jackson, S. Schmitt, Q.P. Dou, J.J. Kodanko, Synthesis, characterization, and reactivity of the stable iron carbonyl complex [Fe(CO)(N4Py)](ClO4)2: photoactivated carbon monoxide release, growth inhibitory activity, and peptide ligation, Inorg. Chem. 50 (2011) 5336–5338, https://doi.org/10.1021/ic200676s.

[94] R.N. Perutz, B. Procacci, Photochemistry of transition metal hydrides, Chem. Rev. 116 (2016) 8506–8544, https://doi.org/10.1021/acs.chemrev.6b00204.

[95] W. Wang, T.B. Rauchfuss, L. Bertini, G. Zampella, Unsensitized photochemical hydrogen production catalyzed by diiron hydrides, J. Am. Chem. Soc. 134 (2012) 4525–4528, https://doi.org/10.1021/ja211778j.

[96] R.L. Sweany, Matrix photolysis of tetracarbonyldihydridoiron. Evidence for oxidative addition of dihydrogen on tetracarbonyliron, J. Am. Chem. Soc. 103 (1981) 2410–2412, https://doi.org/10.1021/ja00399a047.

[97] I.E. Buys, L.D. Field, T.W. Hambley, A.E.D. McQueen, Photochemical reactions of [cis-Fe(H)2(Me2PCH2CH2PMe2)2] with thiophenes: insertion into C-H and C-S bonds, J. Chem. Soc. Chem. Commun. (1994) 557–558, https://doi.org/10.1039/C39940000557.
[98] M.V. Baker, L.D. Field, Reaction of ethylene with a coordinatively unsaturated iron complex Fe(DEPE)2: sp2 carbon-hydrogen bond activation without prior formation of a.pi.-complex, J. Am. Chem. Soc. 108 (1986) 7436–7438, https://doi.org/10.1021/ja00283a065.
[99] L.D. Field, A.V. George, B.A. Messerle, Methane activation by an iron phosphine complex in liquid xenon solution, J. Chem. Soc., Chem. Commun. (1991) 1339–1341, https://doi.org/10.1039/C39910001339.
[100] In remembrance of Barnett Rosenberg, Dalton Trans. (2009) 10648–10650, https://doi.org/10.1039/B918993A.
[101] N.J. Wheate, S. Walker, G.E. Craig, R. Oun, The status of platinum anticancer drugs in the clinic and in clinical trials, Dalton Trans. 39 (2010) 8113–8127, https://doi.org/10.1039/C0DT00292E.
[102] J. Chen, J. Stubbe, Bleomycins: towards better therapeutics, Nat. Rev. Cancer 5 (2005) 102, https://doi.org/10.1038/nrc1547.
[103] W.A. Wani, U. Baig, S. Shreaz, R.A. Shiekh, P.F. Iqbal, E. Jameel, A. Ahmad, S.H. Mohd-Setapar, M. Mushtaque, L. Ting Hun, Recent advances in iron complexes as potential anticancer agents, New J. Chem. 40 (2016) 1063–1090, https://doi.org/10.1039/C5NJ01449B.
[104] K. Woodburn, Chemical Aspects of Photodynamic Therapy By Raymond Bonnett (University of London). Gordon and Breach Science Publishers: London and Newark. 2000. xi + 305 pp. $48.00. ISBN 90-5699-248-1, J. Am. Chem. Soc. 123 (2001) 3622. doi:10.1021/ja0048228.
[105] M. Ethirajan, Y. Chen, P. Joshi, R.K. Pandey, The role of porphyrin chemistry in tumor imaging and photodynamic therapy, Chem. Soc. Rev. 40 (2011) 340–362, https://doi.org/10.1039/B915149B.
[106] I. Ott, R. Gust, Non platinum metal complexes as anti-cancer drugs, Arch. Pharm. (Weinheim) 340 (2007) 117–126, https://doi.org/10.1002/ardp.200600151.
[107] P. Koepf-Maier, H. Koepf, Non-platinum group metal antitumor agents. History, current status, and perspectives, Chem. Rev. 87 (1987) 1137–1152, https://doi.org/10.1021/cr00081a012.
[108] M.J. Clarke, F. Zhu, D.R. Frasca, Non-platinum chemotherapeutic metallopharmaceuticals, Chem. Rev. 99 (1999) 2511–2534, https://doi.org/10.1021/cr9804238.
[109] Q. Li, W.R. Browne, G. Roelfes, Photoenhanced oxidative DNA cleavage with non-heme iron(II) complexes, Inorg. Chem. 49 (2010) 11009–11017, https://doi.org/10.1021/ic1014785.
[110] Q. Li, W.R. Browne, G. Roelfes, DNA cleavage activity of Fe(II)N4Py under photo irradiation in the presence of 1,8-naphthalimide and 9-aminoacridine: unexpected effects of reactive oxygen species scavengers, Inorg. Chem. 50 (2011) 8318–8325, https://doi.org/10.1021/ic2008478.
[111] Q. Li, M.G.P. van der Wijst, H.G. Kazemier, M.G. Rots, G. Roelfes, Efficient nuclear DNA cleavage in human cancer cells by synthetic bleomycin mimics, ACS Chem. Biol. 9 (2014) 1044–1051, https://doi.org/10.1021/cb500057n.
[112] A. Garai, U. Basu, I.L.A. Pant, P. Kondaiah, A.R. Chakravarty, Polypyridyl iron (II) complexes showing remarkable photocytotoxicity in visible light, J. Chem. Sci. 127 (2015) 609–618, https://doi.org/10.1007/s12039-015-0815-0.
[113] L. Tabrizi, Novel cyclometalated Fe(II) complex with NCN pincer and BODIPY-appended 4′-Ethynyl-2,2′:6′,2″-terpyridine as mitochondria-targeted photodynamic anticancer agents, Appl. Organomet. Chem. (2017) e4161, https://doi.org/10.1002/aoc.4161.
[114] M. Roy, B. Pathak, A.K. Patra, E.D. Jemmis, M. Nethaji, A.R. Chakravarty, New insights into the visible-light-induced DNA cleavage activity of dipyridoquinoxaline complexes of bivalent 3d-metal ions, Inorg. Chem. 46 (2007) 11122–11132, https://doi.org/10.1021/ic701450a.
[115] M.S. Shongwe, C.H. Kaschula, M.S. Adsetts, E.W. Ainscough, A.M. Brodie, M.J. Morris, A phenolate-induced trans influence: crystallographic evidence for unusual asymmetric coordination of an α-diimine in ternary complexes of iron (III) possessing biologically relevant hetero-donor N-centered tripodal ligands, Inorg. Chem. 44 (2005) 3070–3079, https://doi.org/10.1021/ic048835o.
[116] S. Saha, R. Majumdar, M. Roy, R.R. Dighe, A.R. Chakravarty, An iron complex of dipyridophenazine as a potent photocytotoxic agent in visible light, Inorg. Chem. 48 (2009) 2652–2663, https://doi.org/10.1021/ic8022612.
[117] S. Saha, D. Mallick, R. Majumdar, M. Roy, R.R. Dighe, E.D. Jemmis, A.R. Chakravarty, Structure–activity relationship of photocytotoxic iron(III) complexes of modified dipyridophenazine ligands, Inorg. Chem. 50 (2011) 2975–2987, https://doi.org/10.1021/ic1024229.
[118] S. Saha, R. Majumdar, A. Hussain, R.R. Dighe, A.R. Chakravarty, Biotin-conjugated tumour-targeting photocytotoxic iron(III) complexes, Philos. Trans. R. Soc. A Math. Phys. Eng. Sci. 371 (2013), https://doi.org/10.1098/rsta.2012.0190.
[119] A. Garai, I. Pant, P. Kondaiah, A.R. Chakravarty, Iron(III) salicylates of dipicolylamine bases showing photo-induced anticancer activity and cytosolic localization, Polyhedron 102 (2015) 668–676, https://doi.org/10.1016/j.poly.2015.10.026.
[120] U. Basu, I. Khan, A. Hussain, B. Gole, P. Kondaiah, A.R. Chakravarty, Carbohydrate-appended tumor targeting iron(III) complexes showing photocytotoxicity in red light, Inorg. Chem. 53 (2014) 2152–2162, https://doi.org/10.1021/ic4028173.
[121] U. Basu, I. Pant, A. Hussain, P. Kondaiah, A.R. Chakravarty, Iron(III) complexes of a pyridoxal schiff base for enhanced cellular uptake with selectivity and remarkable photocytotoxicity, Inorg. Chem. 54 (2015) 3748–3758, https://doi.org/10.1021/ic5027625.
[122] T. Sarkar, S. Banerjee, A. Hussain, Significant photocytotoxic effect of an iron (iii) complex of a Schiff base ligand derived from vitamin B6 and thiosemicarbazide in visible light, RSC Adv. 5 (2015) 29276–29284, https://doi.org/10.1039/C5RA04207K.
[123] U. Basu, I. Pant, I. Khan, A. Hussain, P. Kondaiah, A.R. Chakravarty, Iron(III) catecholates for cellular imaging and photocytotoxicity in red light, Chem. – An Asian J. 9 (2014) 2494–2504, https://doi.org/10.1002/asia.201402207.
[124] M. Roy, T. Bhowmick, S. Ramakumar, M. Nethaji, A.R. Chakravarty, Double-strand DNA cleavage from photodecarboxylation of ([small mu]-oxo)diiron (iii) l-histidine complex in visible light, Dalton Trans. (2008) 3542–3545, https://doi.org/10.1039/B802533A.
[125] M. Roy, T. Bhowmick, R. Santhanagopal, S. Ramakumar, A.R. Chakravarty, Photo-induced double-strand DNA and site-specific protein cleavage activity of l-histidine ([small mu]-oxo)diiron(iii) complexes of heterocyclic bases, Dalton Trans. (2009) 4671–4682, https://doi.org/10.1039/B901337G.
[126] M. Roy, R. Santhanagopal, A.R. Chakravarty, DNA binding and oxidative DNA cleavage activity of ([small mu]-oxo)diiron(iii) complexes in visible light, Dalton Trans. (2009) 1024–1033, https://doi.org/10.1039/B815215B.
[127] S.B. Chanu, S. Banerjee, M. Roy, Potent anticancer activity of photo-activated oxo-bridged diiron(III) complexes, Eur. J. Med. Chem. 125 (2017) 816–824, https://doi.org/10.1016/j.ejmech.2016.09.090.
[128] T. Sarkar, R.J. Butcher, S. Banerjee, S. Mukherjee, A. Hussain, Visible light-induced cytotoxicity of a dinuclear iron(III) complex of curcumin with low-micromolar IC50 value in cancer cells, Inorg. Chim. Acta 439 (2016) 8–17, https://doi.org/10.1016/j.ica.2015.09.026.
[129] A. Fürstner, Iron catalysis in organic synthesis: a critical assessment of what it takes to make this base metal a multitasking champion, ACS Cent. Sci. 2 (2016) 778–789, https://doi.org/10.1021/acscentsci.6b00272.
[130] W. Nam, Synthetic mononuclear nonheme iron-oxygen intermediates, Acc. Chem. Res. 48 (2015) 2415–2423, https://doi.org/10.1021/acs.accounts.5b00218.
[131] M.J. Collins, K. Ray, L. Que, Electrochemical generation of a nonheme oxoiron (IV) complex, Inorg. Chem. 45 (2006) 8009–8011, https://doi.org/10.1021/ic061263i.
[132] H. Kotani, T. Suenobu, Y.-M. Lee, W. Nam, S. Fukuzumi, Photocatalytic generation of a non-heme oxoiron(IV) complex with water as an oxygen source, J. Am. Chem. Soc. 133 (2011) 3249–3251.
[133] D.W. Low, J.R. Winkler, H.B. Gray, Photoinduced oxidation of microperoxidase-8: generation of ferryl and cation-radical porphyrins, J. Am. Chem. Soc. 118 (1996) 117–120, https://doi.org/10.1021/ja9530477.
[134] J. Berglund, T. Pascher, J.R. Winkler, H.B. Gray, Photoinduced oxidation of horseradish peroxidase, J. Am. Chem. Soc. 119 (1997) 2464–2469, https://doi.org/10.1021/ja961026m.
[135] M.E. Ener, Y.-T. Lee, J.R. Winkler, H.B. Gray, L. Cheruzel, Photooxidation of cytochrome P450-BM3, Proc. Natl. Acad. Sci. 107 (2010), 18783 LP-18786. http://www.pnas.org/content/107/44/18783.abstract.
[136] C.E. Immoos, A.J. Di Bilio, M.S. Cohen, W. Van der Veer, H.B. Gray, P.J. Farmer, Electron-transfer chemistry of Ru–Linker–(Heme)-modified myoglobin: rapid intraprotein reduction of a photogenerated porphyrin cation radical, Inorg. Chem. 43 (2004) 3593–3596, https://doi.org/10.1021/ic049741h.
[137] I. Hamachi, S. Tsukiji, S. Shinkai, S. Oishi, direct observation of the ferric-porphyrin cation radical as an intermediate in the phototriggered oxidation of ferric- to ferryl-heme tethered to Ru(bpy)3 in reconstituted myoglobin, J. Am. Chem. Soc. 121 (1999) 5500–5506, https://doi.org/10.1021/ja984199f.
[138] N.-H. Tran, N. Huynh, T. Bui, Y. Nguyen, P. Huynh, M.E. Cooper, L.E. Cheruzel, Light-initiated hydroxylation of lauric acid using hybrid P450 BM3 enzymes, Chem. Commun. 47 (2011) 11936–11938, https://doi.org/10.1039/C1CC15124J.
[139] N.-H. Tran, D. Nguyen, S. Dwaraknath, S. Mahadevan, G. Chavez, A. Nguyen, T. Dao, S. Mullen, T.-A. Nguyen, L.E. Cheruzel, An efficient light-driven P450 BM3 biocatalyst, J. Am. Chem. Soc. 135 (2013) 14484–14487, https://doi.org/10.1021/ja409337v.
[140] M. Kato, Q. Lam, M. Bhandarkar, T. Banh, J. Heredia, A.U.L. Cheruzel, Selective C–H bond functionalization with light-driven P450 biocatalysts, Comptes Rendus Chim. 20 (2017) 237–242, https://doi.org/10.1016/j.crci.2015.10.005.
[141] S. Fukuzumi, W. Nam, Thermal and photoinduced electron-transfer catalysis of high-valent metal-oxo porphyrins in oxidation of substrates, J. Porphyr. Phthalocyan. 20 (2016) 35–44, https://doi.org/10.1142/S1088424616300032.
[142] M. Ghosh, K.K. Singh, C. Panda, A. Weitz, M.P. Hendrich, T.J. Collins, B.B. Dhar, S. Sen Gupta, Formation of a Room Temperature Stable Fe V (O) Complex : Reactivity, 2014, 40–43.
[143] B. Chandra, K.K. Singh, S. Sen, Gupta, Selective photocatalytic hydroxylation and epoxidation reactions by an iron complex using water as the oxygen source, Chem. Sci. 8 (2017) 7545–7551, https://doi.org/10.1039/C7SC02780J.
[144] C. Herrero, A. Quaranta, M. Sircoglou, K. Senechal-David, A. Baron, I.M. Marin, C. Buron, J.-P. Baltaze, W. Leibl, A. Aukauloo, F. Banse, Successive light-induced two electron transfers in a Ru-Fe supramolecular assembly: from Ru-Fe(ii)-OH2 to Ru-Fe(iv)-oxo, Chem. Sci. 6 (2015) 2323–2327, https://doi.org/10.1039/C5SC00024F.
[145] F. Avenier, C. Herrero, W. Leibl, A. Desbois, R. Guillot, J. Mahy, A. Aukauloo, Photoassisted generation of a dinuclear iron(III) peroxo species and oxygen-atom transfer, Angew. Chem. Int. Ed. 52 (2013) 3634–3637, https://doi.org/10.1002/anie.201210020.

[146] R. Zhang, R.E.P. Chandrasena, E. Martinez, J.H. Horner, M. Newcomb, Formation of compound I by photo-oxidation of compound II, Org. Lett. 7 (2005) 1193–1195, https://doi.org/10.1021/ol050296j.
[147] D.N. Harischandra, R. Zhang, M. Newcomb, Photochemical generation of a highly reactive iron–oxo intermediate. A true iron(V)–Oxo species?, J Am. Chem. Soc. 127 (2005) 13776–13777, https://doi.org/10.1021/ja0542439.
[148] R.M. Richman, M.W. Peterson, Photodisproportionation of.mu.-oxo-bis [(tetraphenylporphinato)iron(III)], J. Am. Chem. Soc. 104 (1982) 5795–5796, https://doi.org/10.1021/ja00385a045.
[149] M.W. Peterson, D.S. Rivers, R.M. Richman, Mechanistic considerations in the photodisproportionation of.mu.-oxo-bis((tetraphenylporphinato)iron(III)), J. Am. Chem. Soc. 107 (1985) 2907–2915, https://doi.org/10.1021/ja00296a013.
[150] M.W. Peterson, R.M. Richman, Photodisproportionation of (.mu.-oxo)bis ((tetrakis(4-carboxyphenyl)porphinato)iron(III), Inorg. Chem. 24 (1985) 722–725, https://doi.org/10.1021/ic00199a018.
[151] B.J. Pistorio, C.J. Chang, D.G. Nocera, A phototriggered molecular spring for aerobic catalytic oxidation reactions, J. Am. Chem. Soc. 124 (2002) 7884–7885, https://doi.org/10.1021/ja026017u.
[152] J.M. Hodgkiss, C.J. Chang, B.J. Pistorio, D.G. Nocera, Transient absorption studies of the pacman effect in spring-loaded diiron(III) μ-Oxo bisporphyrins, Inorg. Chem. 42 (2003) 8270–8277, https://doi.org/10.1021/ic034751o.
[153] J. Rosenthal, B.J. Pistorio, L.L. Chng, D.G. Nocera, Aerobic catalytic photooxidation of olefins by an electron-deficient pacman bisiron(III) μ-oxo porphyrin, J. Org. Chem. 70 (2005) 1885–1888, https://doi.org/10.1021/jo048570v.
[154] J. Rosenthal, T.D. Luckett, J.M. Hodgkiss, D.G. Nocera, Photocatalytic oxidation of hydrocarbons by a bis-iron(III)-μ-oxo pacman porphyrin using O2 and visible light, J. Am. Chem. Soc. 128 (2006) 6546–6547, https://doi.org/10.1021/ja058731s.
[155] S.K. Ghosh, R. Patra, S.P. Rath, Synthesis, structure and photocatalytic activity of a remarkably bent, cofacial ethene-linked diiron (III) μ-oxobisporphyrin, Inorg. Chim. Acta 363 (2010) 2791–2799, https://doi.org/10.1016/j.ica.2010.03.005.
[156] I.M. Wasser, H.C. Fry, P.G. Hoertz, G.J. Meyer, K.D. Karlin, Photochemical organic oxidations and dechlorinations with a μ-oxo bridged heme/non-heme diiron complex, Inorg. Chem. 43 (2004) 8272–8281, https://doi.org/10.1021/ic0490932.
[157] D.N. Harischandra, G. Lowery, R. Zhang, M. Newcomb, Production of a putative iron(V)–oxocorrole species by photo-disproportionation of a bis-corrole–diiron(IV)–μ-oxo dimer: implication for a green oxidation catalyst, Org. Lett. 11 (2009) 2089–2092, https://doi.org/10.1021/ol900480p.
[158] A. Draksharapu, Q. Li, G. Roelfes, W.R. Browne, Photo-induced oxidation of [FeII(N4Py)CH3CN] and related complexes, Dalton Trans. 41 (2012) 13180–13190, https://doi.org/10.1039/c2dt30392b.
[159] G. Roelfes, M. Lubben, R. Hage, J. Que, B.L Feringa Lawrence, Catalytic oxidation with a non-heme iron complex that generates a low-spin FeIIIOOH intermediate, Chem. – A Eur. J. 6 (2000) 2152–2159, https://doi.org/10.1002/1521-3765(20000616)6:12<2152::AID-CHEM2152>3.0.CO;2-O.
[160] S.L. Esarey, J.C. Holland, B.M. Bartlett, Determining the fate of a non-heme iron oxidation catalyst under illumination, oxygen, and acid, Inorg. Chem. 55 (2016) 11040–11049, https://doi.org/10.1021/acs.inorgchem.6b01538.
[161] J. Chen, A. Draksharapu, E. Harvey, W. Rasheed, L. Que, W.R. Browne, Direct photochemical activation of non-heme Fe(IV)O complexes, Chem. Commun. 53 (2017) 12357–12360, https://doi.org/10.1039/c7cc07452b.
[162] J. Chen, S. Stepanovic, A. Draksharapu, M. Gruden, W.R. Browne, A non-heme iron photocatalyst for light-driven aerobic oxidation of methanol, Angew. Chem. Int. Ed. 57 (2018) 3207–3211, https://doi.org/10.1002/anie.201712678.
[163] J. Chen, D. Unjaroen, S. Stepanovic, A. van Dam, M. Gruden, W.R. Browne, Selective photo-induced oxidation with O 2 of a non-heme iron(III) complex to a bis(imine-pyridyl)iron(II) complex, Inorg. Chem. 57 (2018) 4510–4515, https://doi.org/10.1021/acs.inorgchem.8b00187.